Taxonomic reassessment of the Little pocket mouse, *Perognathus longimembris* (Rodentia, Heteromyidae) of southern California and northern Baja California

James L. Patton[1]*, and Robert N. Fisher[2]

[1] Museum of Vertebrate Zoology, 3101 Valley Life Sciences Building, University of California, Berkeley, CA 94720, USA. Email: patton@berkeley.edu.
[2] U.S. Geological Survey, Western Ecological Research Center, 4165 Spruance Road, Suite 200, San Diego, CA 92101, USA. Email: rfisher@usgs.gov.
* Corresponding author: https://orcid.org/0000-0002-8709-7196.

The Little pocket mouse (*Perognathus longimembris*) encompasses 15 to 16 currently recognized subspecies, six of which are restricted to southern California and adjacent northern Baja California. Using cranial geomorphometric shape parameters and dorsal color variables we delineate six regional groups of populations from this area that we recognize as valid, but these differ in name combination and geographic range from the current taxonomy. We resurrect two names from their current placement in synonymies, synonymize two currently recognized subspecies, and we reassign a third. Importantly, we restrict the U. S. Federally endangered Pacific pocket mouse (*P. l. pacificus* Mearns) to the vicinity of its type locality at the mouth of the Tijuana River in the southwestern corner of San Diego County and resurrect *P. l. cantwelli* von Bloeker for the other two population segments along the coast, those that span the northwestern corner of San Diego County and adjacent Orange County and that in coastal Los Angeles County. The name *cantwelli* would now apply to the only extant populations of the Pacific pocket mouse, a reassignment with obvious management implications. Our taxonomic decisions also reconfigure the ranges of other subspecies of conservation concern, notably *P. l. bangsi* Mearns and *P. l. brevinasus* Osgood.

Para el ratón de abazones menor (*Perognathus longimembris*) se tienen reconocidas quince o dieciséis subespecies, de las cuales seis de ellas tienen una distribución restringida al sur de California y la parte colindante del norte de Baja California. Haciendo uso de parámetros geométricos de la forma craneal y variables en la coloración dorsal, delimitamos y reconocimos como válidos seis grupos regionales de poblaciones, los cuales difieren en el nombre y área geográfica de su actual clasificación taxonómica. Reincorporamos dos nombres de las actuales sinonímias, combinamos dos subespecies que se encuentran actualmente reconocidas y reasignamos una tercera. Es importante destacar que para el ratón de abazones menor (*P. l. pacificus* Mearns), que se encuentra en peligro de extinción a nivel federal de E.U.A., restringimos su distribución a la vecindad de su localidad tipo en la boca del Río Tijuana, localizada en la esquina suroeste de San Diego County. Asimismo, reincorporamos a la subsepcie *P. l. cantwelli* von Bloeker a los otros dos segmentos de la población a lo largo de la costa, abarcando la esquina noroeste de San Diego County, colindante con Orange County y la costa de Los Angeles County. El nombre *cantwelli* ahora se aplicaría a las únicas poblaciones del ratón de bolsillo del Pacífico, un reasignamiento con notorias impicaciones en su manejo. Nuestras decisiones taxonómicas también incluyen la reconfiguración en los rangos de otras subespecies que son preocupantes para la conservación, como lo son *P. l. bangsi* Mearns y *P. l. brevinasus* Osgood.

Introduction

The Little pocket mouse, *Perognathus longimembris* Coues, occupies desertscrub habitats throughout the Great Basin, Mojave, Colorado, and western parts of the Sonoran deserts in western North America (Hall 1981). It also has a very limited occurrence in the California Floristic Province (CFP) along the Pacific coast in California (Cooper 1869). Infraspecific taxonomy has not been reviewed across the entire range since Osgood (1900); the only treatments subsequent to the last subspecies description (Hall 1941) are those for taxa occurring within Nevada (Hall 1946), Utah (Durrant 1952), and Arizona (Hoffmeister 1986). Of the 22 nominal taxa assigned to the species, recent taxonomic synopses have recognized either 15 (Patton 2005) or 16 (Williams *et al.* 1993; Hafner 2016) as valid, treating the remainder as synonyms. A thorough review of the species using modern morphological and molecular approaches is long overdue and also the subject of a larger review of the complex by one of us (JLP and collaborators).

Herein we examine the morphological disparity of Little pocket mice in one relatively small area of the species' range, that across southern California and adjacent northern Baja California. In part, our treatment serves as a companion to available mitochondrial DNA views of population diversity across this same region (Swei *et al.* 2003). It also, hopefully, will serve as a taxonomic guidepost for population-level genomic studies now initiated by researchers at the San Diego Zoo Wildlife Alliance (Wilder *et al.* 2022) and the University of California Museum of Vertebrate Zoology, through the California Conservation Genomics Project

(https://www.ccgproject.org/) and a refocus on taxa and areas of conservation concern for coordinated management decisions at the local, state, and federal levels.

Our area of interest includes six currently recognized subspecies: *aestivus* Huey, *bangsi* Mearns, *bombycinus* Osgood, *brevinasus* Osgood, *internationalis* Huey, and *pacificus* Mearns. This number represents 37.5 to 40 % of the valid infraspecific taxonomic diversity within *P. longimembris* but represents only about 10 % of the total species' range (approximately 22,000 mi^2 compared to 213,000 mi^2). Despite the small encompassing area, high taxonomic diversity across this region is perhaps not surprising, as was found in a larger analysis of mammal "evolutionary hotspots" in California (Davis *et al.* 2008). Both ecological and topographic diversity are extreme, with five (of the 17) California ecoregions and four (of 11) geomorphic provinces included all or in part. The area also includes the only U.S. federally endangered pocket mouse (the Pacific pocket mouse, *P. l. pacificus* Mearns), now limited to only two small areas along the central coast in Orange and San Diego counties, and three of five other subspecies listed by the California Department of Fish and Wildlife as State Species of Special Concern, with a rank of S1 (Critically Imperiled) or S2 (Imperiled; CNDDB 2022).

Two of our six target taxa (*pacificus* Mearns and *bombycinus* Osgood) were originally described as distinct species and two were arranged under different specific epithets (*arenicola* Stephens and *brevinasus* Osgood allocated, as subspecies, to *P. panamintinus* Merriam); Williams *et al.* (1993) included all within their concept of *P. longimembris*. These authors also placed *arenicola* Stephens (following Grinnell 1913, 1933 and Huey 1928) and *cantwelli* von Bloeker (following Huey 1939 and Hall 1981) as junior synonyms of *bangsi* Mearns and *pacificus* Mearns, respectively. Of the six taxa Williams *et al.* (1993) treated as valid (*pacificus* Mearns, *bangsi* Mearns, *brevinasus* Osgood, *bombycinus* Osgood, *aestivus* Huey, and *internationalis* Huey), these authors regarded only *internationalis* as of equivocal validity. While California samples along the lower Colorado River are currently assigned to *bombycinus* Osgood (see Grinnell 1913, 1914, 1933; Hall 1981; and Williams *et al.* 1993), the type locality of this taxon is Yuma, Yuma County, Arizona, on the opposite bank. This river forms the dividing line between multiple subspecies and sister species of heteromyid and other rodents (*e. g.*, Grinnell 1914; Hoffmeister and Lee 1967; Riddle *et al.* 2000).

Diversity among population samples of *P. longimembris* across the area has been examined, at least limitedly, by morphological and molecular characters. Over 80 years ago, Huey (1939), for example, compared adult specimens of all forms named above and provided tables of mensural character data, but his analyses were limited by small sample sizes, geographic coverage, and analytical scope. He noted (p. 49), however, while "an ultimate revision of the group" was required that "such a work is, owing to the considerable amount of material yet to be gathered, still in the distant future." At the molecular level, Swei *et al.* (2003) showed that mitochondrial DNA diversity, while extensive within local populations, failed to recover any phylogeographic lineage structure among geographic samples assigned to *pacificus* Mearns, *bangsi* Mearns, *brevinasus* Osgood, and *internationalis* Huey. Species-wide mitochrondrial data now available (JLP, unpublished data) place the California populations allocated to *bombycinus* Osgood within the same mitochondrial group as those reported by Swei *et al.* (2003) yet indicate that this group of subspecies differs from topotypic and other samples of *bombycinus* across the lower Colorado River in Arizona. Unfortunately, no molecular data are yet available for *aestivus* Huey.

Huey's "distant future" is today. The population-level genomic studies mentioned above will undoubtedly inform important issues of demographic history while identifying areas of isolation and/or genetic connectedness among extant populations. Eventually, these studies may also identify the underlying genetic basis for key morphological characters we describe below and provide a window into the role that selection has played in generating that diversity. We include analyses that center on colorimetric as well as standard mensural data of the skin and skull, to allow comparison to the limited published studies, and expand cranial analyses by using two-dimensional geometric morphometric approaches to delineate explicit shape differences. Our goal is to describe disparity among available population samples for each of the six taxa in our study area, to assess if the current taxonomy actually reflects geographically defined patterns of character variation, and to inform conservation understanding and management decisions if not.

Materials and methods

We examined a total of 721 museum specimens, of which we digitized 672 intact, adult skulls from 123 separate localities. These we grouped into 20 geographic samples (map, Figure 1; Appendix 1 provides provenance and catalog numbers) based on preliminary analyses that assigned nearby small samples into larger non-significant subsets as determined by oneway ANOVA and Tukey-Kramer post hoc tests. Seven of these samples comprise only the holotype (*pacificus* Mearns, 1898 [USNM 61022], *bangsi* Mearns, 1898 [MCZ 5304; incorrectly listed as AMNH 5304 in Williams *et al.* 1993], *arenicola* Stephens, 1900 [USNM 99828], *brevinasus* Osgood, 1900 [USNM 186515], *aestivus* Huey, 1928 [SDNHM 6110], *cantwelli* von Bloeker, 1932 [MVZ 74680], and *internationalis* Huey, 1939 [SDNHM 11971]) and topotypes of each of the nominal taxa that have been described from our study area. We initially allocated samples to recognized subspecies following range limits given by Grinnell and Swarth (1913) and Grinnell (1933) rather than by Williams *et al.* (1993), who assigned specimens from San Gorgonio Pass (Banning east to Cabazon) to *P. l. brevinasus* not *P. l. bangsi*. We treated specimens from localities not included within each sample (black circles in Figure 1) as unknown.
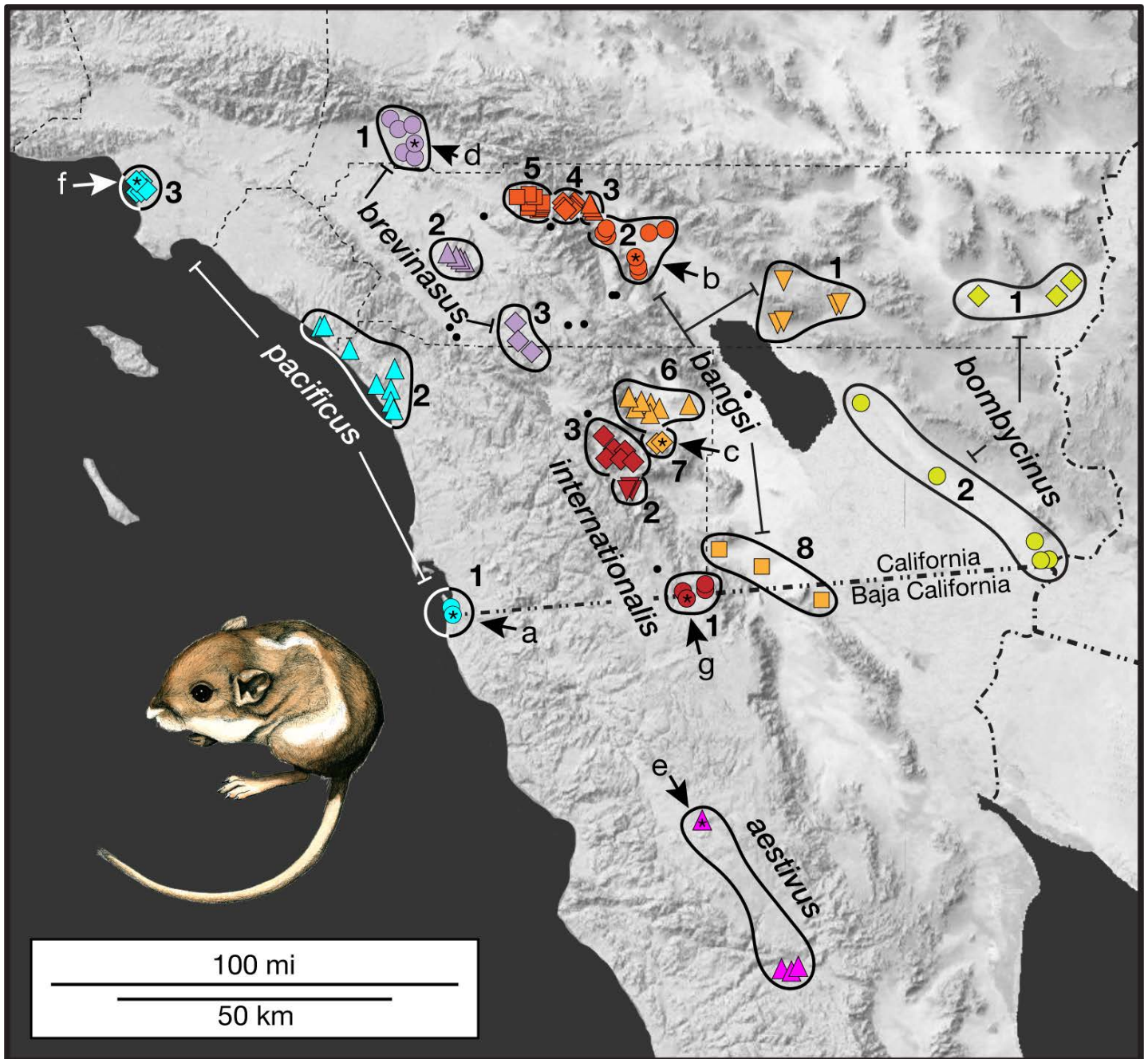
Figure 1. Individual localities allocated to 20 regional samples of *Perognathus longimembris* across southern California and northern Baja California, color coded by subspecies allocation, and population within subspecies by symbol shape. Small black circles are localities with few, mostly singleton, specimens treated as unknown in canonical variate analyses. Arrows and asterisks identify the type locality of each of the seven named taxa allocated to *P. longimembris* in this area (listed by date and page priority: a = *pacificus* Mearns, b = *bangsi* Mearns, c = *arenicola* Stephens, d = *brevinasus* Osgood, e = *aestivus* Huey, f = *cantwelli* von Bloeker, g = *internationalis* Huey). Inset drawing of a Pacific pocket mouse by Tristan Edgarian.

Age criteria. We categorized age classes by maxillary tooth wear similar to the scheme employed by Hoffmeister (1986: Figure 5.131) for Arizona samples of *P. longimembris*, respectively: age class 0 – deciduous premolar 4 still in place or, if gone, permanent PM4 has not reached the molar occlusal plane; age class 1 – PM4 has reached occlusal plane of molar series but all cusps lack evidence of wear; age class 2 – cusps of PM4 and M1-M3 exhibit wear but remain separate or, if partially coalesced, have not unified into complete transverse lophs; age class 3 – cusps of posteroloph of PM4 and anterior and posterior lophs of M1 and M2 have coalesced into separate lophs that remain uncon-

nected on their lingual boundary; age class 4 – anterior cusp of PM4 has coalesced with the posteroloph, lophs of M1-M3 are connected at their lingual border; and age class 5 – the occlusal surface of all teeth are "dished", with enamel present only around the tooth's border (occlusal patterns for age classes 2-5 are illustrated in Figure 2c).

Age classes 0 and 1 are considered to be juvenile animals based on porous auditory bullae and unfused basicranial sutures; age class 0 individuals are uniformly still in juvenile pelage and, for those specimens for which necropsy data are available, had not attained sexual maturity (i.e., females with thin and translucent uteri and males with

very small, non-vascularized testes). Age class 1 individuals varied from still in juvenile pelage, in molt, or already with adult pelage; available necropsy data indicate that none had reached reproductive maturity. All specimens in age classes 2 through 5 had adult pelage and, especially in spring months, nearly all specimens with necropsy data exhibited signs of present or recent reproductive activity (females with enlarged, swollen uteri, embryos present, or embryo scars visible; males with enlarged, scrotal, and vascularized testes, and enlarged vesicular glands).

Non-geographic variation. To examine sex and age effects, we performed generalized least squares analyses of the 32 linear distance measurements for adult specimens of two samples: pacificus-1 (type and topotypes of *pacificus* Mearns; $n = 66$) and pacificus-3 (type and topotypes of *cantwelli* von Bloeker; $n = 78$). Application of Bonferroni corrections for multiple comparisons yielded no detectable sexual dimorphism nor significant interaction terms in either sample; significant age effects were found for four variables (nasal length, zygomatic breadth, upper incisor breadth, and mesopterygoid width) only in the pacificus-1 sample (Appendix 2). As a result, we combined sexes and ages in all analyses.

Cranial morphological character sets. We photographed the dorsal and ventral aspects of each skull examined using a Nikon D3200 or Nikon D850 digital camera fitted with AF-S AV Micro Nikkor 105 mm lens. Establishing a common plane for all photographed skulls is essential, whether photographs are used to calculate traditional linear measurements or digitized landmarks for geometric morphometrics. To maintain planar uniformity across specimens, we used a bubble level placed on the camera viewfinder and the platform upon which the skull was placed. For the dorsal view, the ventral surfaces of the bullae and the incisor tips established a common 3-point plane. A common plane for the ventral surface was more difficult to establish, as skulls were too small to use a bubble level laid across the molar rows, for example, and the age-related flattening of the dorsal profile made positioning each skull in a consistent position difficult. We thus placed each skull on a bit of putty and positioned the toothrows to a horizontal plane by eye. Damaged skulls that precluded digitizing all landmarks or accurate measurements, such as those with chipped incisors or broken parts, were excluded.

We digitized 28 landmarks (LM) on the dorsal surface of the skull and 25 on the ventral surface (Figure 2a, b) using the on-line XYOM-CLIC module (http://xyom-clic.eu/; Dujardin and Dujardin 2019). Most landmarks were Type 1 in Bookstein's (1991) terminology – those where the intersection of bony sutures is locally defined; others conform to Type 2 as per Bookstein – those defined, for example, by the tip of a structure (dorsal LM 9, L26) or bulge (LM 6). In addition, we placed 21 semilandmarks (SL) along the lateral border of the auditory capsule, nine SL with uniform spacing between LM 13 and 14 along the edge of the epitympanic portion and 12 between LM 14 and 15 on the edge of the mastoid portion.

We then used MorphoJ, version 1.07a (Klingenberg 2011; available at https://morphometrics.uk/MorphoJ_page.html) to generate matrices of Procrustes coordinates, or residuals, that result from superimposition, and principal components of the set of Procrustes residuals (or relative warp scores). MorphoJ uses the latter in canonical variate comparisons of a priori defined samples and to compute matrices of Mahalanobis distances among them. We also used MorphoJ to construct wireframes (sets of lines linking landmarks in a predetermined configuration) and deformation grids to visualize shape changes among taxon samples.

We also took 20 linear measurements from the dorsal surface, including the area (mm²) of the bullar capsule, and 12 measurements from the ventral surface from each skull photograph using ImageJ, version 1.46r (Abramoff *et al.* 2004; Schneider *et al.* 2012; available at http://imagej.nig.gov/if/download.html). ImageJ measurements were given to three decimals; these we rounded to two places, which is consistent with repeated measures of the same variable. Dorsal variables included: occipital-nasal length (1-ONL – midline distance from distal tip of ex-supraoccipital to anterior tip of nasal bones); nasal length (2-NL – midline length of nasal bones); frontal length (3-FL – midline length of frontal bones); parietal length (4-PL – midline length of parietal bones); interparietal length (5-IPL – midline length of interparietal bone); premaxilla tip length (6-premax-ExtL – midline measurement from the distal nasal bones to a line tangential to the two distal premaxillary extensions); rostral width (7-RW – width across the anterior rostrum at the nasal-premaxillary boundary); maxillary width (8-MW – width across the posterior rostrum at the maxillary-premaxillary boundary); premaxillary extension width (9-premax-tipW – width across the most distal portion of the premaxillary distal extensions); interorbital constriction (10-IOC – least width across the interorbital region); zygomatic breadth (11-ZB – maximum width across the zygomatic arches); anterior parietal width (12-antParietalW – maximum width of the parietal bones at their suture junction with the frontal and squamosal elements); anterior interparietal width (13-IPW-ant – maximum width taken at the suture junction with the parietal and ex-supraoccipital); posterior interparietal width (14-IPW-post – maximum width taken across the posterior corners of the interparietal); ex-supraoccipital width (15-exOccW – width across the exposed ex-supraoccipital elements); bullar width (16-bullarW – maximum width across the two bullae); bulla length (17-bullaL – maximum length from the anterior portion of the epitympanic and posterior portion of the mastoid portions); bulla width (18-bullaW – perpendicular width across the left bulla from the epitympanic-mastoid junction to the inner border with the ex-supraoccipital and parietal); bulla perimeter (19-bulla perimeter – the distance of a line circumscribing the left bulla); bulla area (20-bulla area – calculated for the area circumscribed by bulla perimeter, in mm²). Ventral variables included: anterior nasal extensions (21-anterior border of the upper incisors to the tip of the nasal bones); palatal length (22-posterior border of upper incisors to anterior end of mesopterygoid fossa);

mesopterygoid length (23-anterior end of fossa to a line tangential to the posterior end of the hamular processes); foramen magnum length (24-midline measurement); maxillary toothrow length (25-alveolar length from upper premolar to third molar), incisor breadth (26-alveolar distance from the lateral margins of the incisors); palatal breadth (27-width across outside of maxilla between first and second molars); squamosal width (28-distance between the squamosal extensions); distal width of mesopterygoid (29-across the end of the hamular processes); stylomastoid foramina width (30-across the two stylomastoid foramina), occipital condyle width (31-across the distal ends of each condyle); ex-supraoccipital width (32-distance between the lateral projections of left and right ex-supraoccipital bones). External measurements of total length (TOL), tail length (TAL), hindfoot length, including claw (HF), and ear length, from notch (E) were taken from specimen labels; we calculated head-and-body length (HBL) by subtracting TAL from TOL.

We obtained dorsal and ventral landmark datasets for all digitized specimens of each taxon, although the final number in each differs slightly after removal of outliers. Sample sizes for ventral measurements were often smaller than those from the dorsum due to damaged structures (*e. g*., the hamular processes). In general, we employed linear variables primarily for comparisons to previously published studies that reported differences in cranial dimensions or to test character differences identified in diagnoses of taxa when initially described or subsequently compared.

Dorsal color measurement. Of the 721 specimens examined, 565 had preserved skins. These we photographed to obtain measures of the three Commission internationale de l'éclairage (CIE) color variables L* (lightness, measured on a scale from 0 [= black] to 100 [= diffuse white]), a* (the position on the color spectrum between red/magenta and green [negative values indicate green while positive values indicate magenta]), and b* (the position on the color spectrum between yellow and blue [negative values indicate blue and positive values indicate yellow]). To obtain these values, we first took photographs of the dorsal aspect of each skin at a distance of 25 cm using a Nikon DX SWM micro 1:1 lens and under standard lighting conditions at 4600°K; each photograph was then manipulated to yield an approximate uniform white background with L* = 90, a* = 0, and b* = 1. We then recorded, and averaged, color values at three points along the mid-dorsum from each specimen using the Lab Color Mode in Adobe PhotoShop CC™ (Adobe Systems Inc., San Jose, California). Since pelage color at any spot on the dorsum is variable due to a mixture of dark brown or black intertwined with yellow, individual measurements were an average of a 5 x 5 pixel area.

We converted values of a* and b* to C* (chroma, or relative saturation, which is measured on a scale from 0 to 100), as the square root of $a^{*2} + b^{*2}$, and h° (hue, or angle of the hue in the CIELab color wheel), measured as the arctangent of (b*/a*). A red hue is at 0°, yellow at 90°, green at 180°, and blue at 270°, with orange, yellow-green, cyan, and magenta at 45°, 135°, 225°, and 315°, respectively).
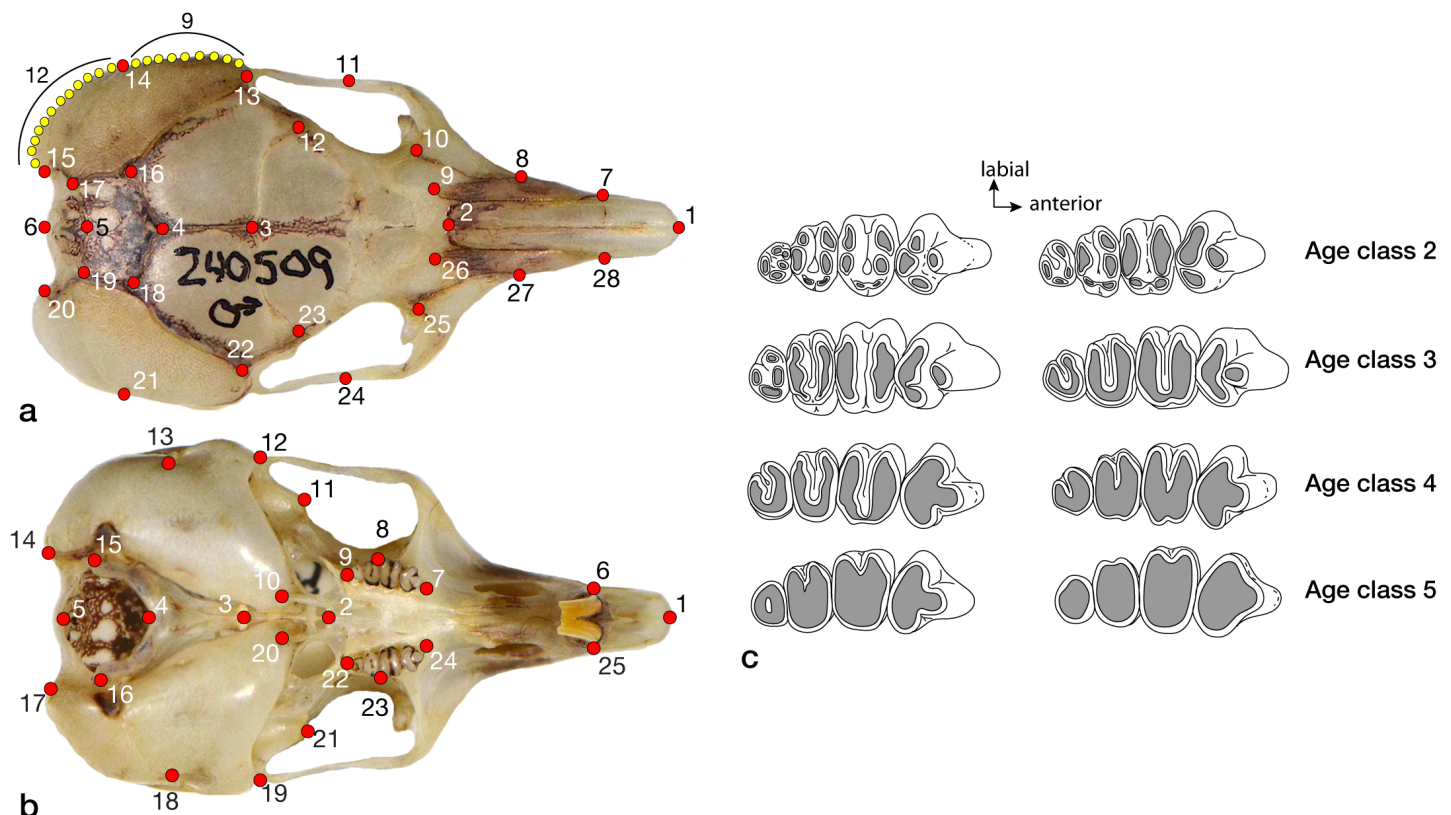

Figure 2. (a) Dorsal view of a skull of *Perognathus longimembris* (MVZ 240590; from East Stone Cabin Valley, Nye Co., Nevada) illustrating the position of 28 dorsal landmarks (LM – red circles) and the 21 semilandmarks (SL – yellow circles) that define the outer margin of the epitympanic (9 SL, black arc) and mastoid (12 SL, black arc) portions of the auditory bulla; (b) ventral view of the same skull with the positions of the 25 ventral landmarks indicated; and (c) maxillary toothrow occlusal surface wear age classes.

Statistical procedures. We performed all multivariate analyses of landmark-semilandmark coordinates in MorphoJ but used JMP Pro16™ (SAS Institute Inc., Cary, North Carolina) for univariate character or multivariate specimen score comparisons among samples for morphometric and colorimetric data. We used oneway ANOVAs followed by Tukey-Kramer pairwise post hoc tests (with Bonferroni corrected *P*-values for multiple comparisons) in all comparisons of samples to delimit non-significant sample subsets. We also used the hierarchical clustering routine in JMP Pro16, with the Ward algorithm, to generate dendrograms from matrices of sample Mahalanobis distances and the canonical variates routine to obtain posterior probabilities for assignment for unknown specimens, those not allocated a priori to one of the 20 samples. The latter provided an unbiased assessment of each specimen phenetic relationship to a priori samples based on posterior probabilities of assignment. As multivariate ordinations of dorsal and ventral landmark datasets yielded similar patterns of sample dispersion in multivariate space, we present only those derived from the dorsal landmarks and semilandmarks. We performed all MorphoJ canonical analyses with permutation tests for pairwise distances with 10,000 iterations. The LSID for this publication is: urn:lsid:zoobank.org:pub:83CCE2F4-CE8C-4DB7-8116-50C83DA819F2.

Results

We begin by using the 32 linear variable dataset to examine character differences among the seven samples, which include the respective holotype and set of topotypes, or near-topotypes, of each nominal taxon in our study area. Here we wish only to evaluate the univariate characters used in the original descriptions or subsequent reviews upon which the current taxonomy has been based. We then examine disparity among all 20 samples mapped in Figure 1 and follow with analyses focused on more limited geographic areas where multivariate patterns of sharp transition are indicated in the global analysis. For these we employ only the dorsal landmark data since, as noted above, both dorsal and ventral landmark data illustrated the same ordination of samples. As we are interested in the phenetic relationships among samples, we only present results from canonical variates analyses.

Cranial characteristics of type and topotypic series. There are seven nominal taxa whose type localities are within the geographic area of our study (*aestivus* Huey, *arenicola* Stephens, *bangsi* Mearns, *brevinasus* Osgood, *cantwelli* von Bloeker, *internationalis* Huey, and *pacificus* Mearns), each within a separate sample (aestivus, bangsi-7, bangsi 2, brevinasus-1, pacificus-3, internationalis-1, and pacificus-1, respectively) that also contain the type series (if identified in the original description) and subsequently collected topotypes.

Earlier comparisons among these taxa centered on body and cranial size as well as the degree of mastoid bulla expansion with concomitant changes in lateral width of the interparietal and ex-supraoccipital bones. A few other cranial elements are mentioned in some accounts (for example, length and breadth of the nasals, or rostrum, and interorbital region), but these are limited to specific pairs of taxa and have not been reviewed across them all. In these limited comparisons, however, the series representing *pacificus* Mearns are uniformly stated to be exceedingly small in body and skull, darker in dorsal color, and with much smaller mastoid bullae, much wider interparietals, shorter rostra or nasals, and wider interorbital regions. In contrast, the series representing *aestivus* Huey is notable for being larger in body and cranial size, with much larger and inflated mastoid bullae that give a greater width to the posterior skull while compressing the interparietal into an almost equal-sided pentagon (*e. g.*, Huey 1928). The other taxa fall varyingly with intermediate character states between the extremes represented by *pacificus* and *aestivus*.

Huey (1939:49) noted "structurally, there is found to be an entirely different trend of development" among the taxa he examined. Specifically, in contrasting samples from the coast and interior valleys through this region, he wrote "forms living nearest the ocean, such as *pacificus* near the shores of the Pacific and *bombycinus* … near the shores of the Gulf of California, have the smallest skulls. In fact, the mice themselves are the smallest members of the species. Those occupying the mountain areas are larger and show generally increasing size from north to south. The maximum size of the cranium is found in the specimens of *aestivus*, which occupies the western slopes of the Sierra Juarez and eastern end of El Valle de la Trinidad… Similarly, in the case of altitude, it is found that the greater the elevation, the greater the development of the bullae."

These general observations are upheld in our comparisons among the type-topotypic series, as evidenced by the minimally non-significant sample subsets for external and selected cranial variables, along with character means, standard errors, and sample sizes provided in Appendix 3. In external characters, Mearn's *pacificus* is the smallest in total length (mean = 119.64 mm), but Huey's *aestivus* is largest only in hind foot length (mean 18.83 mm). There is, however, less uniformity among those cranial characters identified by describers and reviewers in the separation of these taxa. Both *pacificus* and *cantwelli* do have the smallest skulls (mean ONL = 19.83 and 19.76 mm, respectively; not significantly different from one another) with especially small bullae, but significantly smaller from one another (mean bulla perimeter = 17.32 and 16.61 mm); the interparietal of *pacificus* is especially wide (mean IPW-ant = 3.85 mm) but that of *cantwelli* is not (mean 3.55 mm). Conversely, *aestivus* does possess the largest skull (mean ONL = 21.57 mm) and largest bullae (mean bulla perimeter = 21.44 mm), significantly so, but shares long nasals with *bangsi* and *internationalis* (mean NL = 7.70 mm versus 7.67 and 7.57) and the narrowest interparietal with *arenicola* (both with mean IPW-ant = 3.10).

Global cranial disparity among all samples. We illustrate differences in dorsal cranial shape in Figure 3a, a biplot of canonical variate scores for the first two CVA axes. Below and to the left of these axes we present deformation grids, with vectors indicating compression or expansion of specific areas of the skull, and wireframe diagrams that compare the resulting shape differences between the most disparate samples aligned on each axis. In Figure 3b, we show the dendrogram of Mahalanobis distances among samples to illustrate hierarchical relationships among them.

The first two CV axes combine to explain 54.8 % of the total pool of variation; each additional axis explains < 8 %. Samples (Figure 3a) are ordered diagonally into three gen-eral groups that align separately on the two axes: (1) all Colorado Desert floor samples of *bangsi* and *bombycinus* plus *aestivus*; (2), interior basin samples of *brevinasus* and *internationalis* along with *bangsi* samples from San Gorgornio Pass; and (3) coastal samples of *pacificus*. The degree of overlap among samples differs but is notably divergent for the southern (pacificus-1) versus central and northern samples (pacificus-2 and -3) of *pacificus*. Both deformation grid and wireframe diagram for CV1 emphasize the correlated expansion of the bulla and compression of the posteromedial portion of the braincase, with the *pacificus* samples sharing a small bulla and wide interparietal and ex-supraoccipital relative to desert samples of *bangsi*, *bomby-*
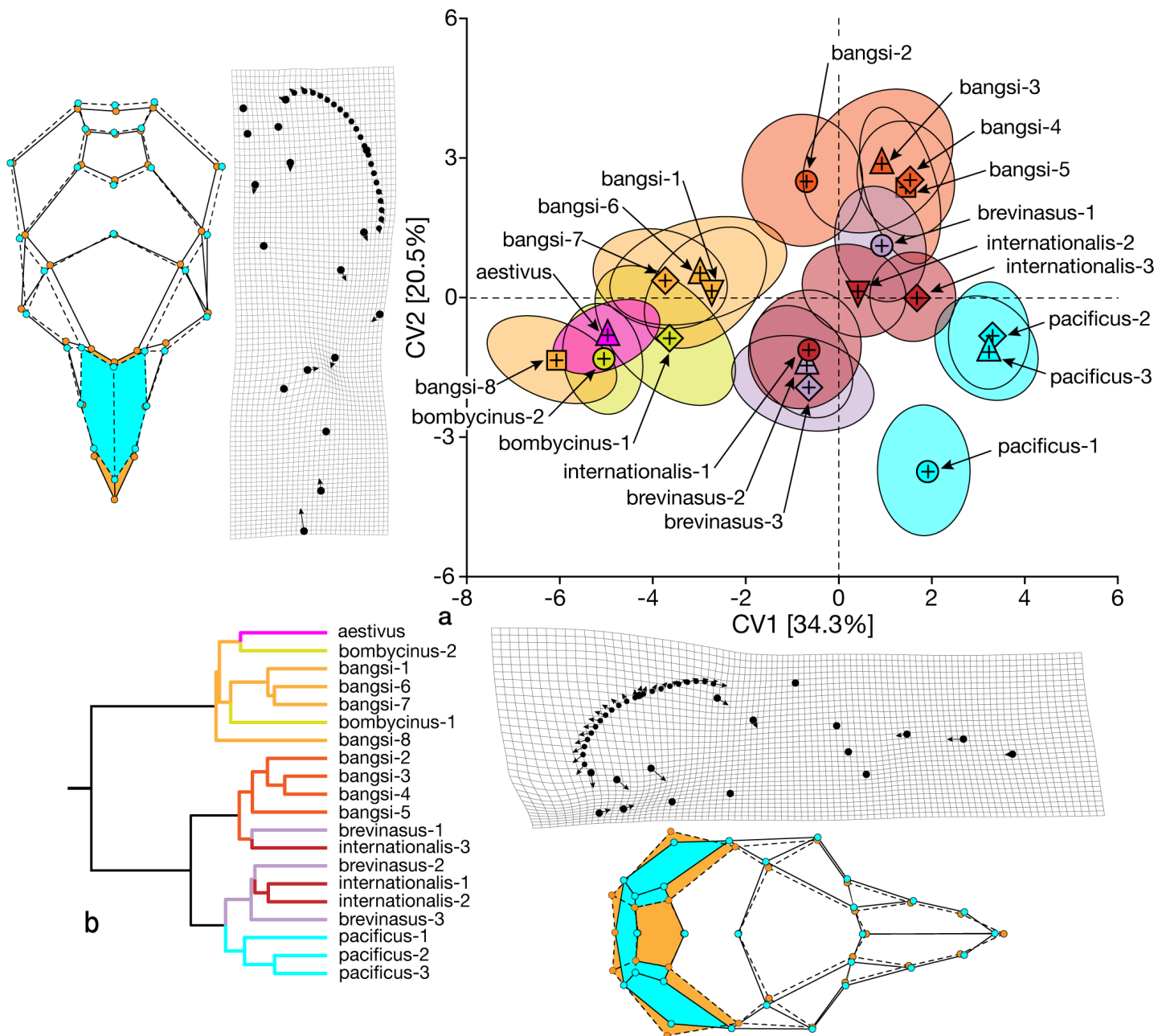

Figure 3. (a) Biplot of canonical variate scores (CV) for the first two axes of dorsal skull landmarks for all 20 samples of *Perognathus. longimembris* from southern California and northern Baja California; data are presented as sample means (+) and ellipses that encompass 50 % of specimen scores. Below and to the left are deformation grids for the left side of the skull, which contains the semilandmarks conforming to the bulla perimeter, and wireframe diagrams of the entire skull, excluding the semilandmarks, with colored highlights of cranial areas of major change that compare samples from the extremes on each axis. (b) Dendrogram of Mahalanobis distances depicting hierarchical similarities among all samples. Symbols and colors are those in the map, Figure 1.

cinus, and *aestivus*. In contrast, CV2 emphasizes shape differences in the rostrum, notably contrasting the elongated nasals and narrowed distal premaxillary tips of *bangsi* samples with short nasals and wider premaxillary tips of *pacificus*. The dendrogram separates samples into the desert samples of *bangsi* (bangsi-1, -6, -7, and -8) and *bombycinus* plus *aestivus* versus all others. The latter is further subdivided, notably with all three *pacificus* samples grouped together, all northern *bangsi* samples (bangsi-2, -3, -4, and -5) grouped, and those allocated to *brevinasus* and *internationalis* split. Centroid size orders samples from largest (*aestivus*) to smallest (all three *pacificus* and the two *bombycinus* samples). Among-sample significant differences are present, but overall samples are ordered from large to small with overlapping non-significant subsets.

The combination of CV1 scores and centroid size ($\log_n CS$; Figure 4) cleanly separates those samples from the desert floor from those of the coast and interior valleys in y-intercept and slope ($z = 5.31$, $P < 0.001$ and 2.19, $P < 0.01$). The single exception is Huey's *aestivus*, which, while occupying the western base of the Sierra Juarez in northern Baja California, shares characteristics of the desert samples. This relationship is contrary to that posited by Huey (1939:49) in his contrast of coastal and interior populations and taxa.

Cranial disparity across transition areas. Three features of the landmark analytical results deserve comment. First, morphological disparity across the entire sample area

reveals two primary groupings of samples: those of the coast, interior valleys, and San Gorgonio Pass and those of the lowland deserts to the east, including the sample from northern Baja California (Figures 3 and 4). Second, there are several geographic areas of sharp transition, both within and between these two geographically structured groups, but also among samples allocated to the same subspecies. And third, samples bordering these sharp transition areas often contain individual specimens that span the mean morphological gap, suggesting phenotypic intermediacy derived from gene flow. Here we examine more closely these transitional areas through CVA. These analyses also permit us to allocate those unknown specimens listed in Appendix 1 by their posterior probabilities to one of the included a priori samples. We organize these analyses by focusing first on transitional areas between the two primary sets of samples identified in figures 3 and 4, specifically (1) *internationalis* versus adjacent *bangsi* samples and (2) *bangsi* versus desert samples. We then consider transitional areas within each of the two global subsets, between (3) coastal *pacificus* versus interior basin *brevinasus* + *internationalis*, (4) *brevinasus* versus *bangsi* samples across San Gorgonia Pass, and (5) northern Baja California *aestivus* versus desert samples of *bangsi* + *bombycinus*. The degree of differentiation across each of these transitions will inform a concluding set of systematic decisions regarding units that warrant taxonomic recognition as well as the geographic range of each. In turn, our
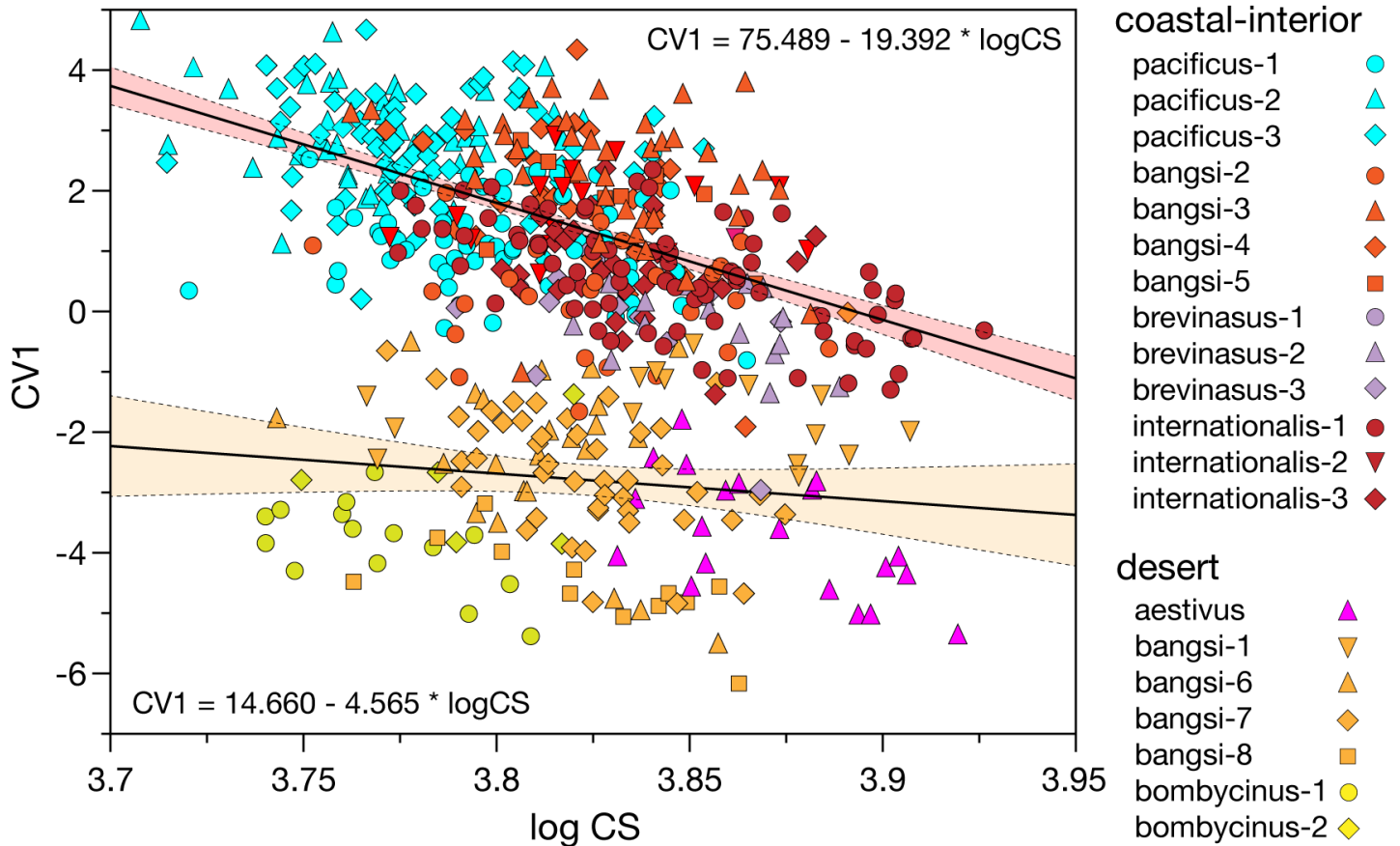

Figure 4. Plot of CV1 scores on log centroid size ($\log_n CS$) for the 20 samples of *Perognathus longimembris* depicted in Figure 3. Regression lines, with 95% confidence limits, and equations are provided. Symbols and colors are those in the map, Figure 1.

suggested taxonomic units will inform conservation status of some, notably *pacificus* and *bangsi*.

1-Southern interior valleys and adjacent desert floor. This area encompasses the phenotypic disparity among the three, southern-most *bangsi* (-6, -7, and -8) and the three *internationalis* samples that are geographically adjacent on the desert floor and interior valleys, respectively (Figure 1). We used the same approach as above, deriving CV scores from CVA in MorphoJ for those specific samples. The combination of CV1 and CV2 scores separates the two taxa on the first axis and orders within-taxon samples geographically (*bangsi* samples from north to south, *internationalis* samples from south to north) on the second (Figure 5a); these two axes combine to explain 70 % of the variation. Samples of *bangsi* have a proportionally longer but posteriorly narrowed rostrum, narrowed frontal and parietal elements, and larger bullae coupled with narrowed interparietal and ex-supraoccipital bones in comparison to those of *internationalis* (see Figure 5a, wireframe diagram). Regression relationships of centroid size (log$_n$CS) on CV1 scores separates the pooled taxon samples (Figure 5b), with significant differences in mean values, y-intercepts, and slopes. The *internationalis* samples are significantly larger in centroid size (pooled *internationalis* log$_n$CS mean = 3.609, pooled *bangsi*

= 3.573; oneway ANOVA $P < 0.001$); the two separate along CV1 (mean eigenvector 1.761 versus -1.952, respectively; $P < 0.001$; y-intercept (34.549 versus -16.504; $P < 0.01$); and slope -9.084 versus 4.073; $P < 0.01$).

The two northern-most *bangsi* samples, however, do broadly overlap with their geographic *internationalis* counterparts, with specimens from each spread across their respective 75 % inclusion ellipses (Figure 5a). This suggests either past and/or present gene exchange between Mason Valley (internationalis-2) and San Felipe Valley (internationalis-3) with San Felipe Narrows (bangsi-7) and Borrego Valley (bangsi-6), perhaps along San Felipe Creek, which connects these areas today. In contrast, there is no overlap of 75 % inclusion ellipses nor are specimens of either misplaced between the southern-most *internationalis* sample (internationalis-1), which contains the holotype and type series from the vicinity of Jacumba, and the few available specimens from localities in the Yuha Desert region that span the international border (bangsi-8). The samples of *bangsi* and *internationalis* thus become progressively more differentiated from north to south along their respective ranges.

2-San Gorgonio Pass and Colorado Desert samples. Here we examine the relationships among samples of *bangsi* Mearns (bangsi-1 through -8) and *bombycinus* Osgood
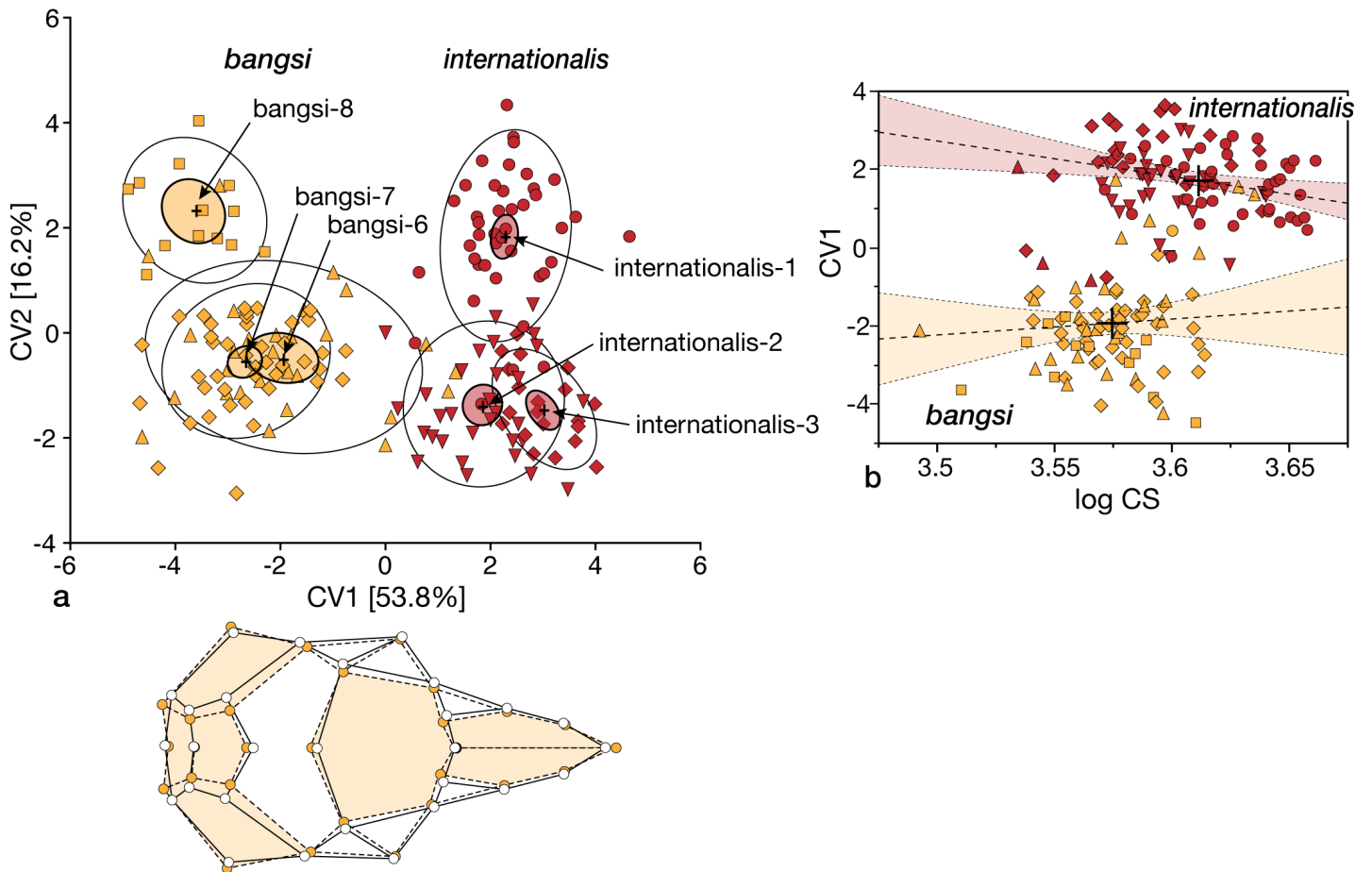

Figure 5. (a) Biplot of canonical variate scores of the first two axes of dorsal cranial landmarks for southern samples of *bangsi* and geographically adjacent samples of *internationalis*; data are presented as sample means (+) and ellipses that encompass 75 % of specimen scores (open ellipses) and 95% confidence limits around the mean (colored ellipses). Below is the wireframe diagram depicting areas of dorsal cranial differentiation highlighted in color comparing *bangsi* (dashed lines, cranial elements in pale orange) with the combined *internationalis* samples (solid lines). (b) Linear regression, with 95% confidence limits, of CV1 scores on log centroid size (log$_n$CS); large crosses indicate mean values. Symbols and colors are those in the map, Figure 1.

(bombycinus-1 and -2) from San Gorgonio Pass east through desertscrub vegetation on the floor of the Colorado Desert of southeastern California (Figure 1). As above, we conducted CVA and illustrate the biplot of CV1 and CV2 scores (which combine to explain 71.2 % of the total variation; note that CV1 alone explains 60.3 %) in Figure 6a. Desert floor samples of *bangsi* and *bombycinus* have much larger bullae that project distally from the occiput and, conversely, laterally compressed interparietal and ex-supraoccipital elements (Figure 6a, wireframe diagram). Regression relationships of centroid size ($\log_n$CS) on CV1 scores again separates the pooled taxon samples (Figure 6b), with significant differences in mean values, y-intercepts, and slopes. San Gorgonio Pass samples of *bangsi* are significantly larger in centroid size (pooled samples bangsi-2 through -5, $\log_n$CS mean = 3.597; pooled desert samples = 3.569; oneway ANOVA $P < 0.001$; the two separate along CV1 (mean eigenvector -2.074 versus 2.547, respectively; $P < 0.001$; y-intercept (-8.695 versus 38.390; $P < 0.05$); and slope 1.840 versus -10.040; $P < 0.01$).

The ordination of samples, however, is less discrete than in the previous transition zone analysis, with broader overlap of specimens among samples from the San Gorgonio

Pass (bangsi-3 through -5) and the geographically adjacent type and topotype series from Palm Springs (bangsi-2). The *bangsi* samples on the desert floor to the immediate east (bangsi-1) and south (bangsi-6 and -7) along the desert side of the Peninsular Ranges overlap partially with the cluster of bangsi-2 through -5, with the two *bombycinus* from the western side of the lower Colorado River, and the bangsi-8 sample from the Yuha Desert region. There is broad overlap between desert floor *bangsi* (bangsi-1, -6, -7, and -8) and the two eastern *bombycinus* samples along the first CV axis. Despite the overlap of adjacent sample individual specimens, there remains clear separations between the northwestern *bangsi* samples (bangsi-2 through -5) and all samples from the floor of the Colorado Desert, with a relatively sharp transition in shape of the distal cranial elements of the bulla, interparietal, and ex-supraoccipital (Figure 6a, wireframe diagram).

3-Coastal versus interior valley samples. This analysis includes the three coastal samples (pacificus-1, -2, and -3) and six from interior valleys (brevinasus-1, -2, -3 and internationalis-1, -2, and 3) that separate from all desert samples further to the east across southern California (see
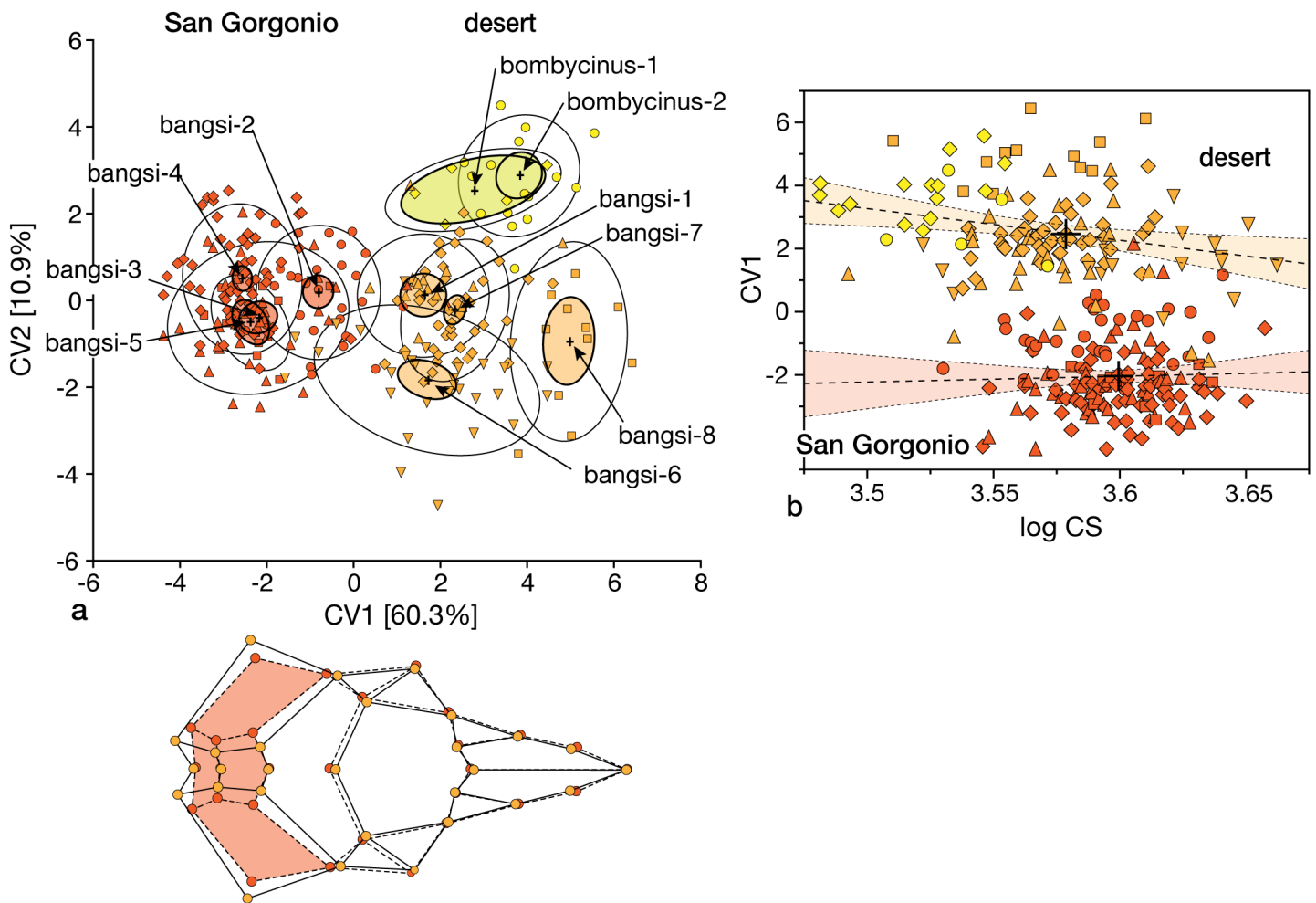

Figure 6. (a) Biplot of canonical variate scores of the first two axes of dorsal cranial landmarks for San Gorgonio Pass and lowland desert samples of *bangsi* and the desert *bombycinus*; data are presented as sample means (+) and ellipses that encompass 75 % of specimen scores (open ellipses) and 95 % confidence limits around the mean (colored ellipses). Below is the wireframe diagram depicting areas of dorsal cranial differentiation highlighted in color comparing northwestern *bangsi* (samples bangsi-2, -3, -4, and 5; dark orange circles, dashed lines, and orange cranial elements) with the combined desert samples of *bangsi* and *bombycinus* (pale orange circles, solid lines). (b) Linear regression, with 95 % confidence limits, of CV1 scores on log centroid size ($\log_n$CS); large crosses indicate mean values. Symbols and colors are those in the map, Figure 1.

Figure 3 and Figure 4). We again used canonical analyses to compare the nine samples and then samples pooled by subspecies allocation (Figure 1). We included all unknown specimens (Appendix 1) to determine their respective assignments in the two analyses.

The first two CVA analyses separate the three coastal samples and those from the interior valleys; for simplicity, we present data for only the 9-group analysis (Figure 7a). The first two axes are nearly equivalent in the percentage of the variation explained (32.1 and 29.1 %, respectively, or 62.2 % combined). While the ordination of samples is similar to that depicted in Figure 3, and with the same cranial features emphasized in this separation (compare wireframe in Figure 7a with that in Figure 3a), the degree of disparity in dorsal shape attributes is much less. These differences, nonetheless, do emphasize the smaller auditory bullae with the laterally expanded interparietal and ex-supraoccipital region along with the short and distally broader rostral elements of the coastal samples, pacificus-1, -2, and -3. Note the distinction between the pacificus-1 (which contains

the type of *pacificus* Mearns) and paired pacificus-2 and -3 samples (the latter which contains the type of *cantwelli* von Bloeker). The two samples of *pacificus* versus *brevinasus* + *internationalis* also differ in their relationship of centroid size ($\log_n CS$) and CV1 scores (Fig 7b; mean $\log_n CS$ coastal = 3.786, interior = 3.838; mean CV1 coastal = 1.483, coastal = -1.620; ANOVA $P < 0.001$ in each comparison), similar to that of the global analysis (Figure 4). In contrast, pooled samples of *brevinasus* and *internationalis* share the same means, y-intercepts, and slopes ($P > 0.05$), with each of those measures, except regression slope, differing from those values for the pooled *pacificus* samples ($P < 0.001$ in each comparison).

Assignments of unknown specimens are unambiguous. The three specimens from San Fernando, Los Angeles County (Appendix 1), are assigned to *pacificus*, specifically sample pacificus-3, at posterior probabilities above 0.948 in the 9-sample and pooled-taxon analyses. In contrast, all specimens from Riverside (Eden Hot Springs, Hemet, Temecula, and Vallevista) and San Diego (McCain Valley and
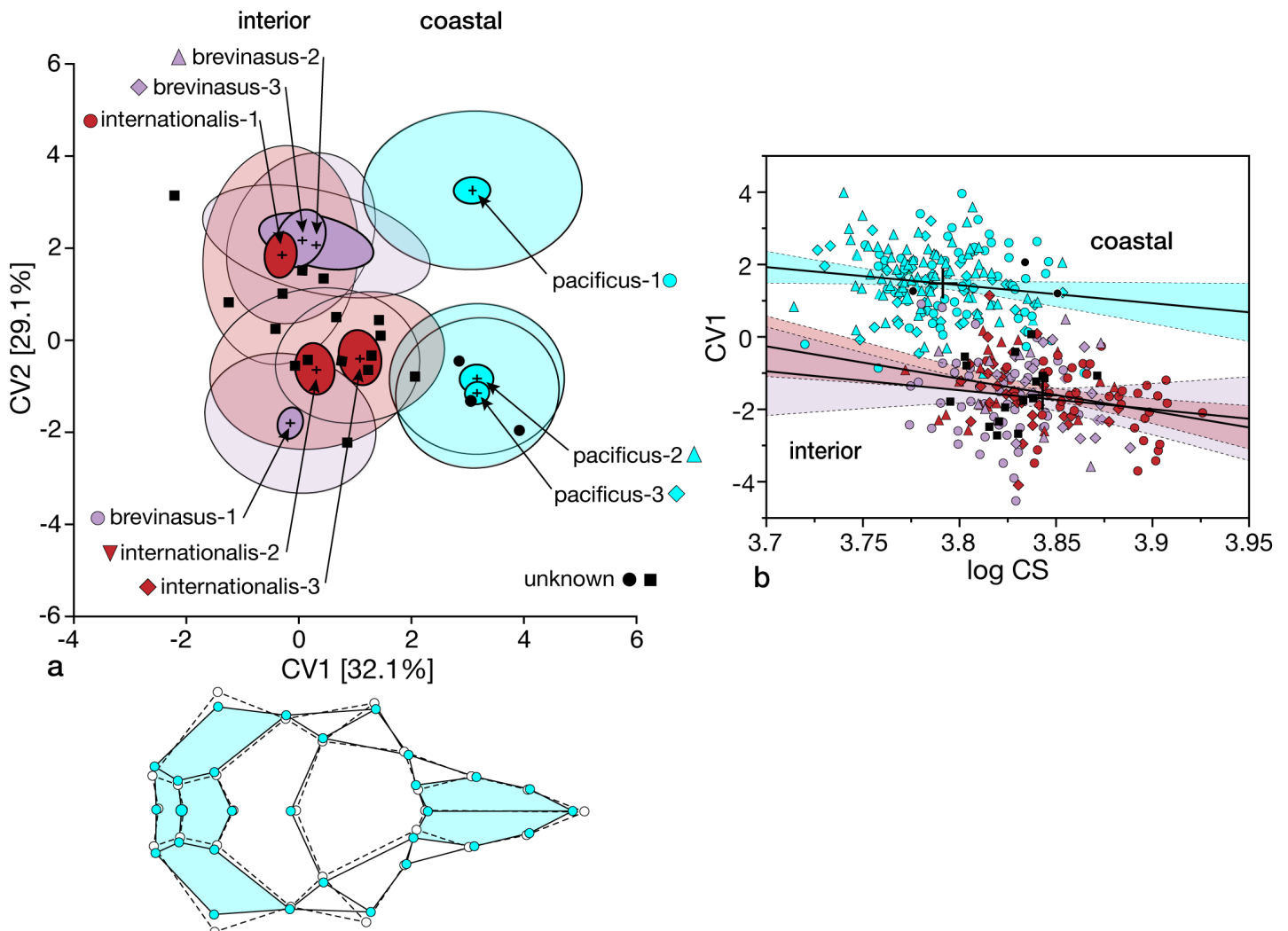

Figure 7. (a) Biplot of canonical variate scores of the first two axes of dorsal cranial landmarks for coastal *pacificus* samples and interior valley samples of *brevinasus*; data are presented as sample means (+) and ellipses that encompass 75 % of specimen scores (open ellipses) and 95 % confidence limits around the mean (colored ellipses). Below is the wireframe diagram depicting areas of dorsal cranial differentiation highlighted in color comparing *pacificus* (solid lines, elements in blue) with the combined *brevinasus* and *internationalis* samples (dashed lines). (b) Linear regression, with 95 % confidence limits, of CV1 scores on log centroid size ($\log_n CS$); large crosses indicate mean values. Symbols and colors are those in the map, Figure 1.

Warner Pass) counties are assigned to the combination of *brevinasus* and *internationalis* samples at posterior probabilities > 0.861. The placement of each is illustrated in Figure 7a, b (black circles are individuals from San Fernando assigned to pacificus-3; black squares are those from Riverside and San Diego counties).

The separation of the three coastal samples into two quite distinct geographic groupings was unexpected. All are currently allocated to the endangered Pacific pocket mouse (*P. l. pacificus*) yet, importantly, all three currently known localities of this mouse are located within the pacificus-2 sample area (two on Camp Pendleton and Dana Point), which aligns with the northern part of this subspecies range (the pacificus-3 sample, which contains the holotype of *cantwelli* von Bloeker) rather than with the southern-most area (pacificus-1 sample) where Mearn's holotype of *pacificus* was collected. We thus wished to ascertain to what degree, if any, the pacificus-2 sample might be divided into southern (pacificus-1 = *pacificus*) and northern (pacificus-3 = *cantwelli*) sets of individuals. We thus performed a CVA with these two sample sets as a priori groups and treated all specimens from the pacificus-2 sample as unknown. Only singleton specimens from either the *pacificus* ($n = 63$, Appendix 1) or *cantwelli* ($n = 78$) samples were misclassified. Among the 48 pacificus-2 specimens, 41 (85.4 %) were assigned to *cantwelli* at posterior probabilities > 0.70 (mean

posterior probability assignment = 0.9796). Seven specimens were assigned to *pacificus* at posterior probabilities of 0.775 or higher (mean assignment = 0.9231). All assignments to *pacificus* came from the southern-most localities in the pacificus-2 sample (Oceanside [3 of 26 specimens], 4 mi N Oceanside [1], Santa Margarita River [1], and Santa Margarita Ranch [2]). The four specimens from the northern-most locality of Dana Point were each assigned to *cantwelli* at posterior probabilities > 0.996.

4-San Gorgonio Pass transect. Here we examine phenetic relationships among the type and topotypic specimens of *brevinasus* from the vicinity of San Bernardino (sample brevinasus-1) east across San Gorgonio Pass (the three samples of *bangsi* from Banning [bangsi-5], Cabazon [bangsi-4], and then Whitewater-Snow Creek [bangsi-3]) plus the type and topotypic specimens of *bangsi* from the vicinity of Palm Springs (bangsi-2). Given differences in subspecies allocation of this set of samples by Grinnell and Swarth (1913; see also Grinnell 1933) and Williams *et al.* (1993), we are specifically interested where phenotypic gaps might be found.

The first two CV axes combined explain 76.4% of the variation (Figure 8a) with the *brevinasus* sample separating from the four samples from San Gorgonio Pass along the first axis and the latter ordered from east (bangsi-2, top) to west (bangsi-5, bottom) on the second axis. Skulls of the different sample sets exhibit more subtle shape differences
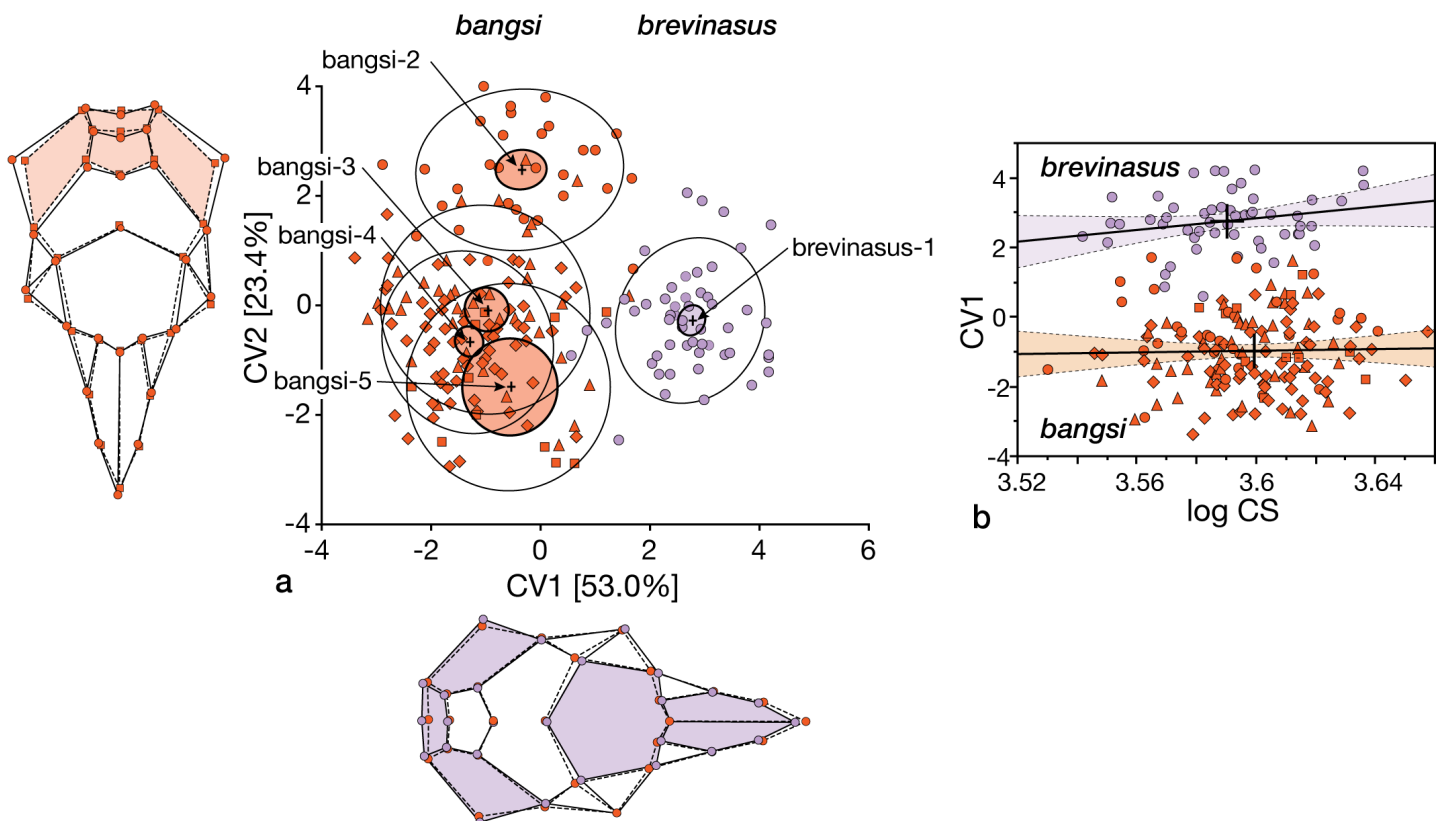

Figure 8. (a) Biplot of canonical variate scores of the first two axes of dorsal cranial landmark for *brevinasus* and *bangsi* samples west to east across San Gorgonio Pass; data are presented as sample means (+) and ellipses that encompass 75 % of specimen scores (open ellipses) and 95 % confidence limits around the mean (colored ellipses). Below is the wireframe diagram depicting areas of dorsal cranial differentiation highlighted in color comparing *brevinasus* (brevinasus-1; purple circles, solid lines, and colored cranial elements) with samples of *bangsi* from the Palm Springs area (bangsi-2) west across those within San Gorgonio Pass (bangsi-3, -4, and -5; orange circles and dashed lines). To the left is the wireframe comparing the bangsi-2 (orange circles and solid lines) sample with the other three (orange squares, dashed lines, and colored cranial elements). (b) Regression plot of CV1 scores on log centroid size ($\log_n$CS). Regression lines, with 95% confidence limits, and equations are provided. Symbols and colors are those in the map, Figure 1.

despite the separation of *brevinasus* from all four *bangsi* samples (Figure 8a, bottom wireframe diagram), with limited specimen overlap between *brevinasus* and its immediate *bangsi* neighbor from the vicinity of Banning (bangsi-5). Differences among the *bangsi* samples along CV2 separate bangsi-2 from the three samples located within San Gorgonio Pass, each geographically adjacent pair of samples with more substantial specimen overlap, mostly by changes in the posterior parts of the skull (bullae, interparietals, and ex-supraoccipitals; Figure 8a, wireframe diagram to the left), the same traits that continue the east to west trend illustrated in Figure 6a. The degree of the *bangsi* sample differences along CV2 is nearly as great as that between the two presumptive subspecies (CV1).

The relationship of centroid size ($\log_n CS$) to CV1 scores separates the sample of *brevinasus* from the pooled samples of San Gorgonio *bangsi* (Figure 8b). The *bangsi* samples are marginally larger in centroid size (pooled *bangsi* $\log_n CS$ mean = 3.598, *brevinasus* = 3.590; one way ANOVA P = 0.03) and the two separate along CV1 (-0.991 versus 2.764, respectively; $P < 0.001$; y-intercept (-5.253 versus -27.453; $P < 0.01$) but not in slope 8.409 versus 1.184; $P > 0.05$).

As a final comment, the type-topotypic series of *brevinasus* (sample brevinasus-1) do not have the shorter nasal bones implied by their name. ANOVA comparisons of the nasal length of brevinasus-1 with each *bangsi* sample in this transect, as well as those of *internationalis*, are universally non-significant (pairwise P-values range from 0.546 to 1.000); in comparison to *pacificus*, *brevinasus* has longer nasals, actually and proportionally ($P < 0.001$ in each comparison).

5-Relationship of aestivus *to desert* bangsi *and* bombycinus. This final set of comparisons focuses on the desert samples of *bangsi* and *bombycinus* plus the northern Baja California *aestivus*, those samples that collectively contrast with coastal and interior ones in a dendrogram of among-sample Mahalanobis distances (Figure 3) and in relationships of their centroid sizes with CV1 scores (Figure 4). Huey (1928:87) diagnosed *aestivus* by its large and inflated mastoid bullae that gave it "a much greater width to the skull posteriorly and compressing the interparietal into an almost equal-sided pentagon." While Huey was certainly correct, these same traits apply to desert *bangsi* samples (the eastern-most bangsi-1 and southern bangsi-6, -7, and 8) as well as the two *bombycinus* samples. The major difference, however, is that the skulls of *aestivus* are largest, *bombycinus* are smallest, and *bangsi* samples are intermediate in size (mean ± standard error for $\log_n CS$: *aestivus* = 3.623 ± 0.006, pooled desert *bangsi* = 3.579 ± 0.003, and pooled *bombycinus* = 3.529 ± 0.006). Furthermore, *aestivus* is broader across the mastoids (bullarW mean = 12.60 mm) than either *bangsi* (range 11.87 mm [bangsi-1] to 11.58 mm [bangsi-6]) or *bombycinus* samples (11.48 mm and 11.33 mm, respectively).

The CVA comparing these seven samples provides limited resolution among them. It takes the first four axes to explain nearly 75 % of the total variation. The first three axes individually explain only 28.5, 18.8, and 15.0 %, respectively. In the biplots of CV1 and CV2 or CV1 and CV3 (Figure 9a, b), most samples align from left to right, along the first CV axis while CV2 and CV3 separate the *aestivus* and one *bangsi* (bangsi-8) samples, respectively. Other combinations of CV axes simply shuffle the positions of these two samples with respect to the core group illustrated in Figure 9 (data not shown). Overall, there is limited resolution on any pair of axes and no clear, well-supported separation among this set of samples.

Pelage color disparity. We provide means, standard errors, sample size, and non-significant sample subsets based on Tukey-Kramer pairwise comparisons in Appen-
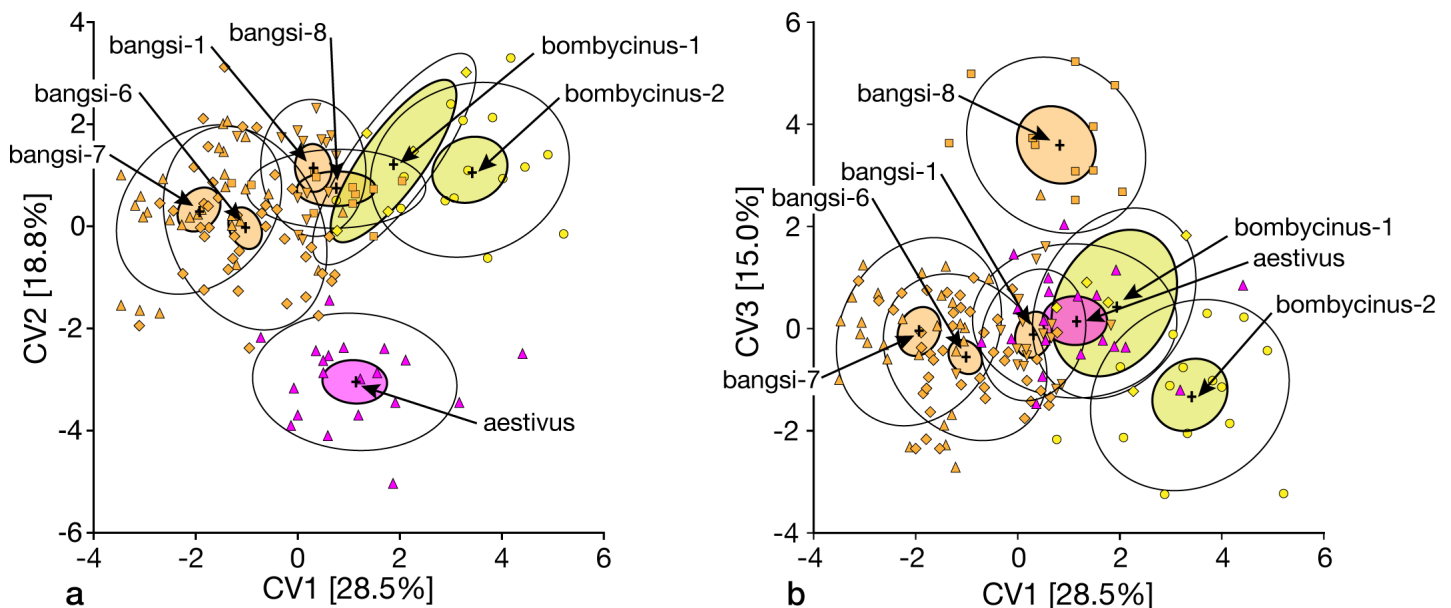
Figure 9. Biplots of canonical variate scores of dorsal cranial landmarks for lowland desert samples of *bangsi* and *bombycinus* plus the northern interior valley sample of *aestivus*; data are presented as sample means (+) and ellipses that encompass 75 % of specimen scores (open ellipses) and 95 % confidence limits around the mean (colored ellipses): A – CV1 and 2 plot; B – CV1 and 3 plot. Symbols and colors are those in the map, Figure 1.

dix 4. All three color variables (lightness, chroma, and hue) vary significantly across the sampled populations (oneway ANOVAs, *P* < 0.001 for each). Lightness varies from quite dark (mean L^* = 13.99 [pacificus-1]) to very pale (46.53 [bangsi-1]) and chroma is ordered in the same way, from lower (in the pacificus-1 sample, mean chroma = 9.442) to higher purity (in bangsi-1, 21.855). Hue varies only negligibly among samples (lowest for pacificus-1 [mean 1.083] and highest in bangsi-6 [1.378]), with all specimens within the red spectrum (sample descriptive statistics in Appendix 3). Overall, the *pacificus* samples differ significantly from interior and, especially, desert samples in all three attributes; visually these are easily distinguished by their very dark overall tones; interior samples are intermediate, and desert ones are distinctly lighter.

In PCA and CVA analyses, the first axis explains the vast majority of the total pool of variation (PC1 = 94.75 %; CV1 = 88.31 %), with lightness the only variable that loads significantly on each axis (PC1 eigenvalue = 0.9541 [versus -0.2996 and -0.0041] for chroma and hue, respectively; CV1 standardized scoring coefficient = 0.9867 [versus 0.0246 and 0.001]). These two multivariate methods display the same ordination of samples, whether these are determined a posteriori (PCA) or a priori (CVA); correlation of specimen PC1 and CV1 scores = 0.998, ANOVA *P* < 0.001. Unsurprisingly, specimen lightness also predicts their individual PC1 and CV1 scores with high efficiency with correlations of 0.997 and 0.999, respectively. One does not need multivariate statistics to see, by eye, differences in pelage lightness among these samples, which we depict as box plots in Figure 10. While some samples are hampered by low numbers of available skins (notably eastern and southern desert bangsi-1 and -8, and bombycinus-1 and -2), the pattern of increasing lightness from coast to desert is obvious. Coastal samples are uniformly darkest but still separate into two significant groups, southern pacificus-1 versus central and northern pacificus-2 and -3 (Figure 10, black bars, which depict non-significant subsets based on Tukey-Kramer HSD). The color separation of these samples mirrors that of their cranial shape (Figs. 3 and 7). Interior basin samples of *brevinasus* and *internationalis*, individually and as a group, are also dark, significantly lighter than coastal *pacificus* but statistically uniform; samples of *bangsi* from west to east across the San Gorgonio Pass form a cline between darker interior and the very light desert samples. Regression of specimen L^* values for the San Gorgonio
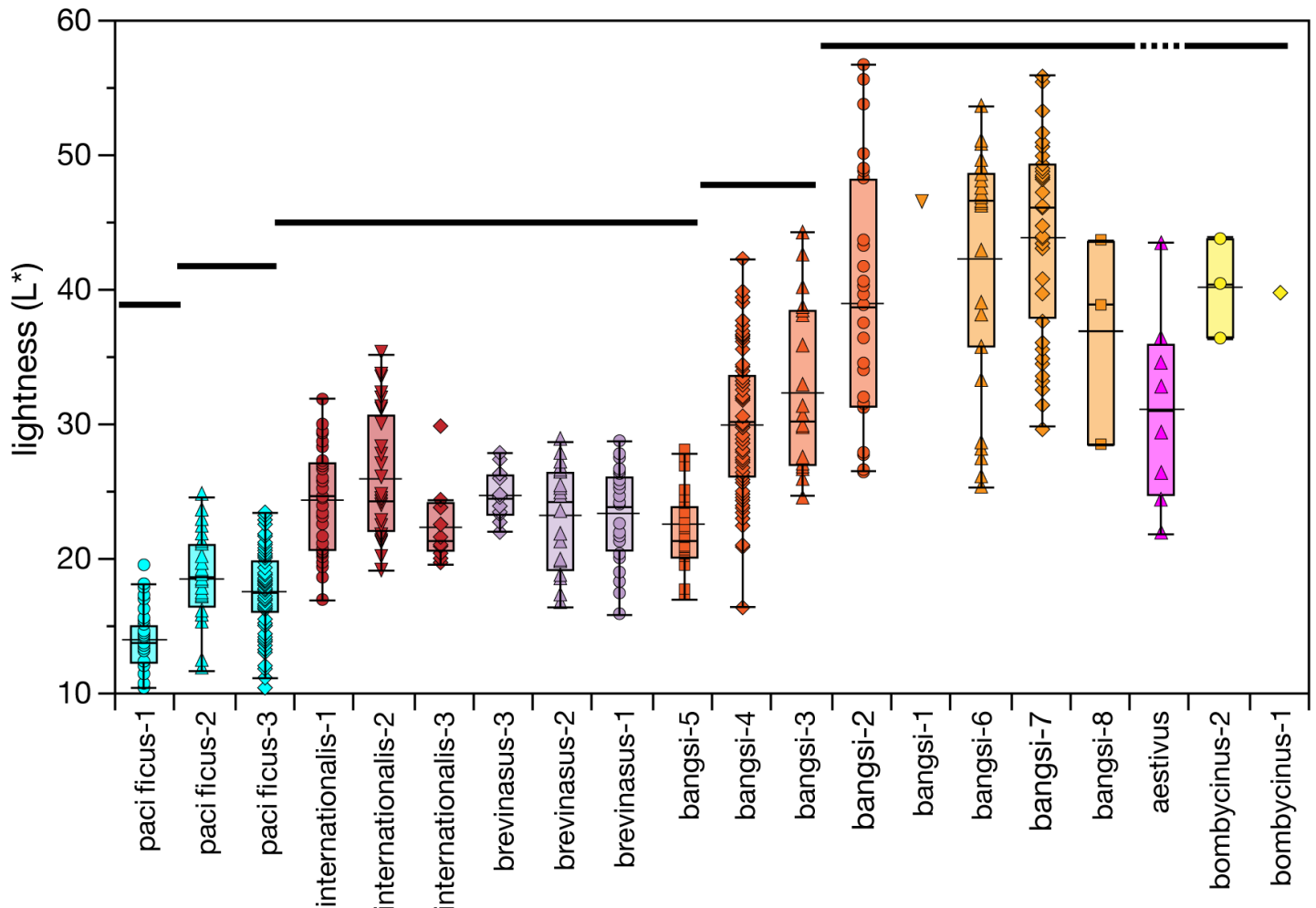
Figure 10. Box plots of pelage lightness, with means and specimen values, for samples of *Perognathus longimembris* from southern California. Samples are arranged from left to right: coastal (*pacificus*), interior valleys (*internationalis* and *brevinasus*), San Gorgonio Pass (*bangsi*, samples 2 through 5), and desert (*bangsi*, samples 1, 6, 7, and -8, *bombycinus*, and including *aestivus* from interior valleys of northern Baja California). Separate heavy lines above samples groups are non-significant subsets (oneway ANOVA, Tukey-Kramer HSD *P* > 0.05). Symbols and colors are those in the map, Figure 1.

Pass localities against longitude is significant (R^2 = 0.307, $df_{1,143}$, F = 62.93, *P* < 0.001). This observation is consistent with [Grinnell and Swarth's (1913](#):360) statement that some specimens from Banning (sample bangsi-5; Figure 1) "show slightly the darkest coloration, perhaps indicating intergradation towards *brevinasus*" and, along with cranial uniformity (Figure 8), support these authors' allocation of specimens from San Gorgonio Pass to *bangsi* rather than to *brevinasus* (contra [Williams *et al.* 1993](#)).

Discussion

We organize this section around two important, and inter-related, components of systematic research. The first addresses broad patterns, and degrees, of cranial and color disparity across the sampled region based on the separate transitional area analyses. This is a necessary first-step before tackling the second component, that of the optimal taxonomy that expresses the disparity of the patterns observed. Following these two components, we then posit historical biogeographic factors that might underly the cranial and pelage color disparities we recovered. We then end with potential management considerations as a result of our suggested taxonomic changes, and with a lament that so much of the original ranges of several of the taxa we include have disappeared under concrete and buildings, or been impacted by recent fires, each of which have changed the landscapes and habitats available for pocket mice and many other organisms, some irreversibly. Nonetheless, we believe it important to describe original patterns and processes of organismal diversification even if these exercises are only depictions of the past, not the future.

Synthesis of morphological disparity among samples. Samples of *Perognathus longimembris* from southern California and northern Baja California are diverse in cranial shape and pelage color, but the patterns are somewhat complex yet still geographically ordered. Here we map (Figure 11a) the major axes of cranial shape differentiation that derive from the global analysis (Figs. 3 and 4) and those of the individual transition areas (Figs. 5 – 9). The major axis of differentiation (heavy solid line in Figure 11a) separates eastern (desert plus *aestivus*) samples from those of the coast and interior valleys. Bridges between these two groups are evident in samples bangsi-2 vis-à-vis adjacent samples bangsi-1 to the east, bangsi-3 to the west, and bangsi-6 to the south (Figure 6), and between bangsi-6 and internationalis-2 (Figure 5). Secondary axes of differentiation occur between samples of coastal *pacificus* relative to the interior *brevinasus* and *internationalis* (Figure 7), and *brevinasus* (from the San Bernardino Valley) and *bangsi* samples (from San Gorgonio Pass; Figure 8). Tertiary levels of divergence occur among the three *pacificus* samples, which separate pacificus-1 (the type and topotypic series) from pacificus-2 and -3 from the central and northern coast, respectively (Figure 7). The array of *brevinasus* and *internationalis* samples, while grouped together, do not exhibit an expected clinal phenetic pattern but rather present as coupled pairs (Figure 7). Eastern

desert samples of *bangsi* and *bombycinus*, including *aestivus*, are collectively less cohesive but, at least with available samples, they are not subdivided (Figure 9).

Dorsal pelage color, dominated by lightness (L*), exhibits the same geographic pattern as cranial shape (compare Figure 10 with Figs. 4 – 9). We have cranial and color data for 358 specimens. For these, we used linear regression to examine the correspondence between individual specimen cranial shape and color CV1 scores (Figure 11b). The relationship between these independent traits is strong (R^2 = 0.4473, df_{1-357}, F = 288.13, *P* < 0.001); specimens from each sample group together and array along the regression line in the consistent coastal to interior to desert pattern.

Taxonomic implications. As the existing subspecific taxonomy implies ([Williams *et al.* 1993](#), [Patton 2005](#), [Hafner 2016](#)), phenotypic diversity across the entire sample area is substantial. In our opinion, available data support the recognition of four to six infraspecific units, listed below, but also a reshuffling of the current assignments of several populations. Coastal *pacificus* possess the most distinctive skull, with its small overall size, very small bullae and concomitant wide interparietals and supraoccipitals, and short rostrum; its recognition should certainly be retained. A lingering question, however, is whether this taxon should be subdivided, with the name *pacificus* Mearns applied only to the area around its type locality in extreme southwestern San Diego County, and *cantwelli* von Bloeker resurrected to encompass the coastal samples in northwestern San Diego and southwestern Orange counties and those around its type locality of Hyperion (= El Segundo) in Los Angeles County. We believe subdivision is warranted as *pacificus* (sensu stricto) and *cantwelli* differ in multiple morphometric, shape, and color attributes, and at a degree consistent with differences among other subspecies recognized (see Figures. 3 and 7, Appendix 3 and 4).

Lacking any clear distinction between the six interior samples into northern and southern units that would map to the current taxa *brevinasus* Osgood and *internationalis* Huey, respectively, as well as the broad overlap among them, we recommend placing both under the earlier described *brevinasus* Osgood. Such action is consistent with the suggestion of equivocal recognition of the two by [Williams *et al.* (1993)](#). We suggest that samples allocated to *bangsi* Mearns be restricted to those in San Gorgonio Pass and the Whitewater River outwash, which includes the type locality of Palm Springs. Even though the type and topotypic series share phenetic similarities with samples to the immediate east (Shavers Valley) and south (Borrego Valley), those relationships are more distant than between the Palm Springs and San Gorgonio Pass samples. Eastern and southern *bangsi* samples, which grade into those allocated to *bombycinus* Osgood in the low eastern desert along the western margin of the lower Colorado River, are best considered a single unit. Given that the type locality of Osgood's *bombycinus* is from Yuma, on the Arizona (eastern) side of the lower Colorado River, samples of which are molecularly and phenotypically
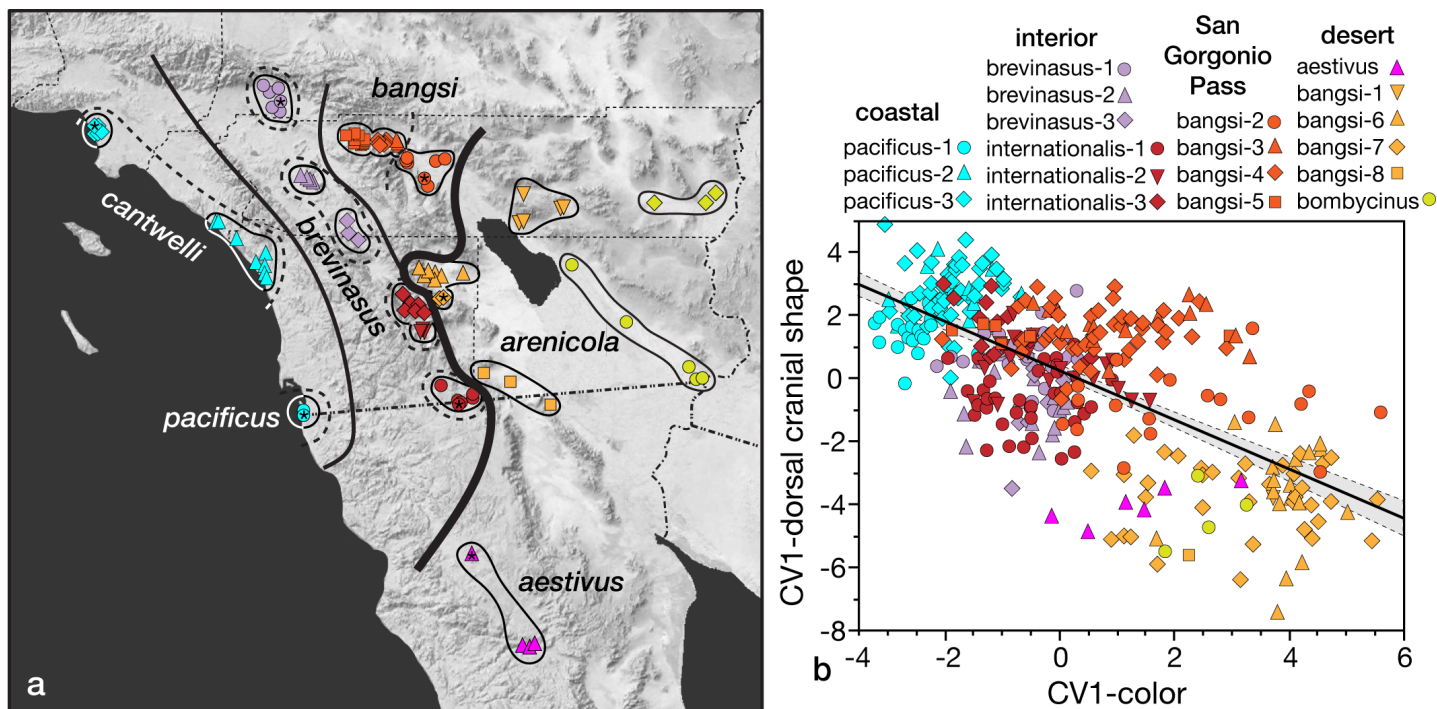
Figure 11. (a) Isophenes of cranial differentiation among samples of *Perognathus longimembris* from southern California and northern Baja California derived from canonical variate analyses presented in Figures 3 through 9. Differentiation is hierarchical, with the heavy line separating regional samples, light solid lines separating units within the western region, and dashed lines separating or grouping samples within current subspecies, but names are provided for infraspecific units we recognize herein. Symbols and colors are those in the map, Figure 1. (b) Regression plot, with 95 % confidence limits around the slope, illustrating the correspondence of individual specimens, as assigned to samples, for dorsal pelage color and cranial shape. Symbols and colors are those in the map, Figure 1.

distinct (JLP, unpublished data), the southeastern California samples cannot be referred to *bombycinus*. Fortunately, the bangsi-7 sample includes the holotype of *arenicola* Stephens; this name is available for these desert populations. As noted by Stephens in his original description, *arenicola* differed from typical *bangsi* by more swollen mastoids that project further posteriorly from the occiput, key features that are demarcated in our analyses (e.g., see wireframe diagram in Figure 6a). Until molecular data are available, we would provisionally retain *aestivus* Huey despite its cranial phenotypic overlap with these desert samples. We note that these suggested rearrangements will impact current conservation strategies for several of these pocket mice. Taxonomy is meant to inform, not to be derivative of those needs. A shortened listing of the valid taxa in southern California and northern Baja California, with range limits, is the following:

Perognathus longimembris pacificus Mearns, 1898

1898. *Perognathus pacificus* Mearns, Bull. Amer. Mus. Nat. Hist., 10:299, 31 August.

1932. *Perognathus longimembris pacificus*: von Bloeker, Proc. Biol. Soc. Washington, 45:127 (first use of current name combination).

Type locality. "Edge of the Pacific Ocean, at the last Mexican boundary monument (No. 258), [San Diego County, California]."

Range. Currently limited to the estuary of the Tijuana River in immediate vicinity of Boundary Monument 258

to 3.2 km north of the monument, San Diego Co., California; likely extends, or used to, even further north along the coast and possibly eastward up the Tijuana River drainage, including into extreme northwestern Baja California, Mexico. Includes localities in sample pacificus-1 (Appendix 1).

Remarks. To our knowledge, this taxon was last collected in the wild in July (von Bloeker 1931b) and October of 1931 (W. H. Burt, Dickey Collection, University of California, Los Angeles).

Perognathus longimembris bangsi Mearns, 1898

1898. *Perognathus longimembris bangsi* Mearns, Bull. Amer. Mus. Nat. Hist., 10:300, 31 August.

1900. *Perognathus panamintinus bangsi*: Osgood, N. Amer. Fauna, 18:29.

Type locality. "Palm Springs, Colorado Desert [Riverside Co.], southern California."

Range. Limited to San Gorgonio Pass (the vicinity of Banning east to Cabezon, Snow Creek, and Whitewater) and outwash of the Whitewater River to the vicinity of Palm Springs, Riverside Co., California. Includes localities of samples bangsi-2, bangsi-3, bangsi-4, and bangsi-5. Localities from San Gorgonio Pass were allocated to *brevinasus* Osgood by Williams *et al.* (1993) but to *bangsi* by Grinnell and Swarth (1913); some, but not all, specimens from Banning share the darker pelage characteristic of that subspecies but cranially pool with other *bangsi* samples from the Pass.

Perognathus longimembris arenicola Stephens, 1900

1900. *Perognathus panamintinus arenicola* Stephens, Proc. Biol. Soc. Washington, 13:153, 13 June.

1918. P[*erognathus*]. l[*ongimembris*]. *arenicola*: Osgood, Proc. Biol. Soc. Washington, 31:96 (first use of current name combination).

Type locality. "San Felipe Narrows, San Diego Co., California."

Range. Colorado Desert of eastern California and northeastern Baja California, from Shavers Valley east to Blythe (Riverside County) and Borrego Valley south to the Yuha Basin and east to Pilot Knob (Imperial County); range in Baja California unclear but probably extends south along the coast of the Sea of Cortez at least to San Felipe. Includes localities in samples bangsi-1, bangsi-6, bangsi-7, bangsi-8, bombycinus-1, and bombycinus-2.

Remarks. Treated as a synonym of *P. l. bangsi* by Grinnell (1913, 1933), Hall (1981), and Williams *et al.* (1993). May include *aestivus* Huey, pending molecular data if and when available. Grinnell (1914) assigned specimens from the vicinity of Pilot Knob to *P. l. bombycinus*, the type locality of which is in Arizona (see above).

Perognathus longimembris brevinasus Osgood, 1900

1900. *Perognathus panamintinus brevinasus* Osgood, N. Amer. Fauna, 18:30, September.

1928. *Perognathus longimembris brevinasus*: Huey, Trans. San Diego Soc. Nat. Hist., 8:88 (first use of current name combination).

1939. *Perognathus longimembris internationalis*: Huey, Trans. San Diego Soc. Nat. Hist., 9(11):47. 31 August; type locality "Lower California side of the International Boundary at Jacumba, San Diego County, California," Baja California.

Type locality. "San Bernardino, [San Bernardino Co.], Cal. [California]." Stated by Grinnell (1933) to be "about 2 miles east of present city center."

Range. Interior valleys of southern California from the vicinity of the type locality in San Bernardino County successively south through the interior San Jacinto, Menifee, Aguanga, Oak Grove, Warner, San Felipe, Mason, and McCain valleys to the Jacumba Valley that straddles the international border. Includes localities in samples brevinasus-1, -2, and -3, and internationalis-1, -2, and -3. For assignment of specimens from localities across San Gorgonio Pass (Williams *et al.* 1993) see comment under *P. l. bangsi*.

Perognathus longimembris aestivus Huey, 1928.

1928. *Perognathus longimembris aestivus* Huey, 1928, Trans. San Diego Soc. Nat. Hist., 5:87, 18 January.

Type locality. "Sangre de Cristo in Valle San Rafael on the western base of the Sierra Juárez, Lower [Baja] California, Mexico (upper Sonoran zone), lat. 31° 52′ north, long. 116° 06′ west."

Range. Known only from the type locality and Valle de la Trinidad (localities listed in sample *aestivus*).

Perognathus longimembris cantwelli von Bloeker, 1932.

1869. *Perognathus parvus*, Cooper, Amer. Nat., 3:183

1932. *Perognathus longimembris cantwelli* von Bloeker, Proc. Bio. Soc. Washington, 45:128, 9 September.

1939. *Perognathus longimembris pacificus*: Huey, Trans. San Diego Soc. Nat. Hist., 9(11):49 (first use of synonymy for *cantwelli*).

Type locality. "Hyperion [= El Segundo], Los Angeles County, California."

Range. Currently known from two disjunct areas along the coast of southern California: (1) from Oceanside (San Diego Co.; see von Bloeker 1931b, Bailey 1939) north to Dana Point (Orange Co.; Swei *et al.* 2003) and continuing to Newport in the San Joaquin Hills historically (M'Closkey 1972,; Meserve 1976) and (2) the vicinity of the type locality south along the coast to Wilmington (Cooper 1869) but herein extended to include specimens from San Fernando, Los Angeles County, that others had previously assigned to *P. l. brevinasus* (*e. g.*, von Bloeker 1932; Grinnell 1933; Huey 1939; Williams *et al.* 1993). These two areas correspond to samples pacificus-2 and -3, respectively. When describing this form, von Bloeker (1932) referred the San Fernando samples to *P. l. brevinasus* based on skull characteristics and size although he pointed out it was like his *cantwelli* based on color.

Remarks. Treated as a valid subspecies by Grinnell (1933:148) but as a synonym of *P. l. pacificus* Mearns by most subsequent authors (*e. g.*, Hall 1981; Williams *et al.* 1993). So far as known, today this taxon is limited to small areas on Camp Pendleton Marine Corps Base (San Mateo/San Onofre, and Oscar One and Edson training areas, San Diego County) and Dana Point (Orange County). Bailey (1939) kept two living individuals collected at Oceanside in August of 1931 at his home; one died in December 1935 (Bitty) and the other (Bobbity) on 29 June 1937; see photographs (Figure 12) and accompanying poem, below.

Coming together, falling apart, and loss. The populations of *Perognathus longimembris* we studied form a natural monophyletic group that invaded the Pacific Plate and the Salton Sea trough (Rift Zone) from the east on the Continental Plate, where the species is much more widespread, and then diversified into multiple taxa in various habitat types (Swei *et al.* 2003 and herein). There are multiple other taxa that spread to the Pacific Plate and then diversified; an excellent example is within the plethodontid salamander *Batrachoseps major* complex (Jochsuch *et al.* 2020; see also Gottscho 2016). This contrasts with the *Perognathus parvus* complex that is widespread to the northeast in the Great Basin but only gets into southern California on the rim of the Continental Plate where it diversified (*i. e.*, *Perognathus alticola*) but didn't invade the Pacific Plate at all (Riddle et al. 2014). Reptiles also have multiple lineages in southern California that are specialized for psammophilus habitats; *Perognathus longimembris* is the best example of a small

mammal that shares this niche (Mosauer 1932). These reptile species tend to show regional speciation patterns due to the regionalization of habitats; they serve as useful hypotheses to test our taxonomy (Wood *et al.* 2008; Leaché *et al.* 2009; Parham and Papenfuss 2009; Gottscho *et al.* 2017). Thus, within the Pacific Plate and Rift Zone these mice segregate clearly into five well defined habitat features, and six taxa: San Gorgonio Pass-Coachella Valley (*bangsi*), Colorado Desert (*arenicola*), interior northern Baja valleys (*aestivus*), headwater washes (*brevinasus*), and coastal dunes, washes, and marine terraces (*pacificus* and *cantwelli*). Below we evaluate the biogeography of these major habitat features. Next, we provide a brief history of the focal distributional areas of these mice.

1-San Gorgonio Pass-Coachella Valley: This area at the upper end of the San Andreas Rift Zone is part of the Whitewater-San Gorgonio River system and is bounded on the south by the head of the Salton Trough, and is a region identified in multi-species genetic hotspots analyses (Davis *et al.* 2008; Wood *et al.* 2013). There were expansive dunes in this landscape and high levels of endemism across taxa including additional mammals like the ground squirrel, *Xerospermophilus tereticaudus chlorus*. For psammophilus

reptiles the best example is *Uma inornata* that is restricted to this area but also the snake *Chionactis annulata/occipitalis* that was shown to have a high endemic divergence here as well (Wood *et al.* 2008, 2014; Gottscho *et al.* 2017). Various invertebrates also show high levels of endemism to the dunes and washes including the beetle *Dinacoma caseyi* and the cricket *Ammopelmatus cahuilaensis* (Tinkham 1968; Rubinoff *et al.* 2020). Thus, our revised definition of *P. l. bangsi* geographically fits well within this landscape with high endemism of dune evolved species.

2-Colorado Desert: This area borders the Salton Sea (Lake Cahuilla) on both sides and extends into desert valleys around Anza Borrego and the dune fields bordering the Chocolate Mountains and across to the Chuckwalla Valley but does not cross the Colorado River; rather, it heads south towards San Felipe in Baja California. Little pocket mice were probably continuous across the basin prior to the 1905 flood that formed the present Salton Sea. This area was also identified in Wood *et al.* (2013); the species most closely overlapping *P. l. arenicola* in distribution is the lizard *Uma notata* (Gottscho *et al.* 2017). Much of the northeastern part of the mouse's range is bounded by the Bouse Formation (Buising 1990). There are genetic breaks in two
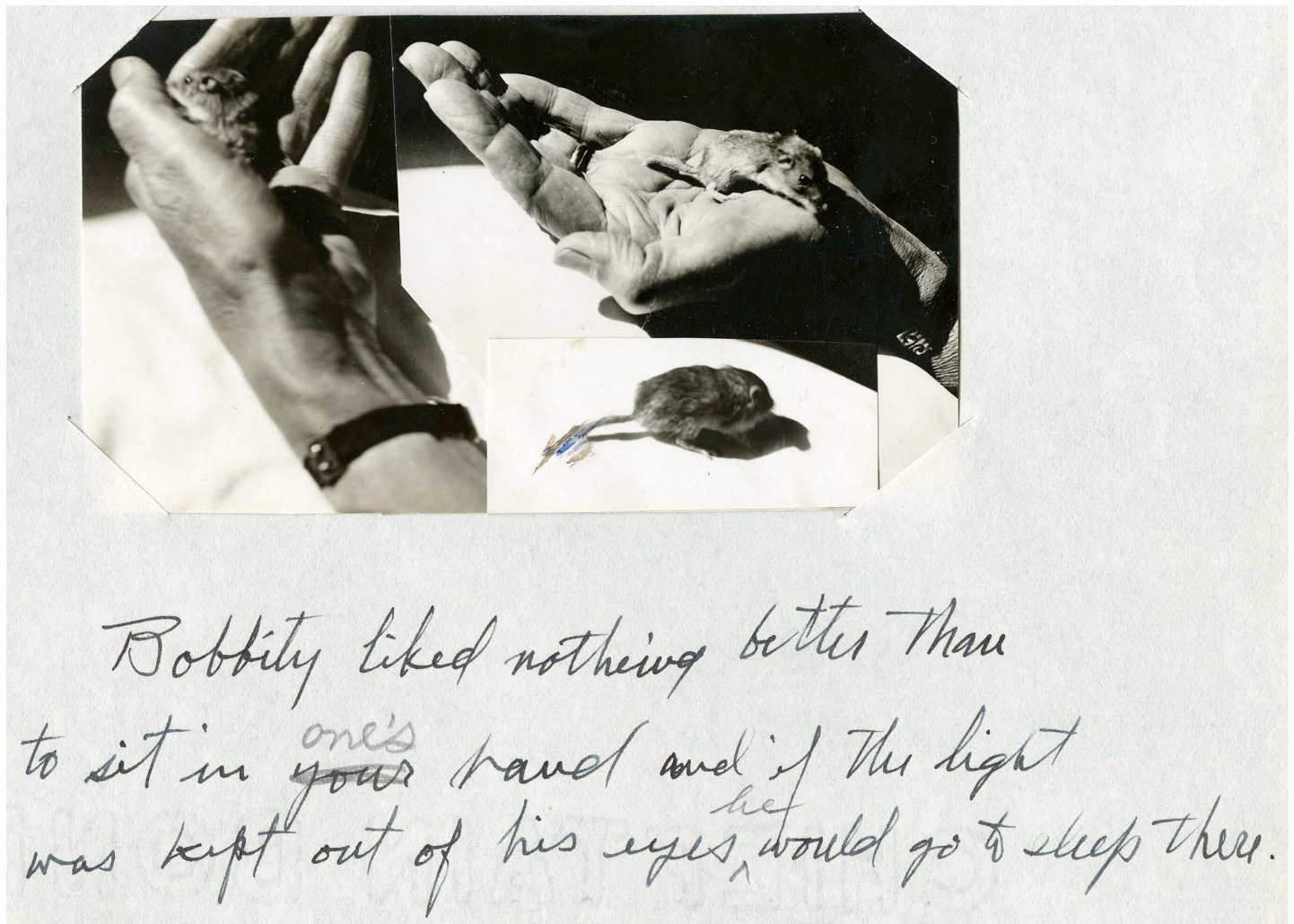

Figure 12. Photographs of Bobbity, Vernon Bailey's pet *P. l. cantwelli* collected at Oceanside, San Diego County on 20 August 1931 and that died on 29 June 1937 at a weight of "26 navy beans" (V. Bailey fieldnotes, Mammal Division archives, National Museum of Natural History, Smithsonian Institution, Washington, D.C.).

different species of horned lizards that match well with this landscape (*Phrynosoma mcallii* and *Phrynosoma platyrhinos*) and occupy the pocket mouse habitats ([Mulcahy *et al.* 2006](#)). The San Andreas fault-line passes through here but both sides of the rift zone are occupied by the same taxa. The eastern margin is the lower Colorado River, which forms a barrier for some taxa, including *P. l. arenicola* and other heteromyids as noted above, but not all. Both *Phrynosoma mcallii* and *Chionactis annulata* cross the river into the Yuma Desert and eastward to the Pinacate region in Sonora, Mexico (*e. g.*, [Mulcahy *et al.* 2006](#); [Wood *et al.* 2014](#)).

3-Interior northern Baja California valleys: The Trinidad and Ojos Negros/San Rafael valleys are connected to the lower part of the Colorado Desert region via the Paseo de San Matias where there is leakage from the desert to these inland xeric valleys for many taxa ([Grismer 1994](#)). The darker pelage of *P. l. aestivus* appears convergent with the darker coloration of the *P. l. brevinasus* further north in similar headwater wash situations on both sides of the Peninsular Ranges. Other desert species leak into these valleys from the desert such as the reptiles *Sceloporus magister*, *Xantusia wigginsi,* and the mammal *Dipodomys merriami trinidadensis* ([Lidicker 1960](#); [Grismer 1994](#); [Álvarez-Castañeda *et al.* 2009](#)). Although these valleys are on the western aspect of the Baja California Peninsula they maintain a more xeric landscape then other coastal areas in northern Baja California. Other valleys to the north and west seem to have appropriate habitat for *Perognathus longimembris* but lack records (Guadalupe Valley and Valle de las Palmas) despite field work conducted by prominent field mammalogists including S. B. Benson, L. M. Huey, and F. Stephens.

4-Headwater washes: These are a set of alluvial fans/basins that extend from north to south along the higher slopes of the Transverse and Peninsular ranges on both coastal and desert slopes. The distribution of *P. l. brevinasus* extends south along the western slope in the upper Santa Ana, Santa Margarita, and San Luis Rey rivers but switches to the eastern slope of the Peninsular Ranges along San Felipe Creek, Vallecito Creek, and Carrizo Creek washes terminating near Jacumba and Mountain Springs on both sides of the international boundary. It is separated spatially from *P. l. arenicola*, occurring at higher elevations within the mountains in appropriate habitat rather than on the Colorado Desert floor. Although this subspecies occurs on coastal and desert slopes, it maintains its phenology along this distribution. A surprising spatial gap in distribution is in the foothills of the San Gabriel Mountains where *P. l. brevinasus* terminates in the west around Etiwanda Wash rather than extending farther to Cucamonga or San Antonio washes where seemingly continuous and appropriate habitats occur. The lack of records from this area across to the San Fernando Valley supports the break we find in our morphologic assessment, where specimens from San Fernando (Lower Big Tujunga Wash) are assigned to *P. l. cantwelli* and not *P. l. brevinasus*. Evidence that this gap is real comes from [MacMillen's (1964)](#) Ph.D. thesis studies in

the San Antonio alluvial fan and our recent trapping work at San Antonio and lower San Gabriel River washes where we also failed to detect any *Perognathus longimembris*. In the northern part of its range, *P. l. brevinasus* closely tracks the highly endemic and endangered San Bernardino kangaroo rat (*Dipodomys merriami parvus*) in the Santa Ana Watershed, then overlaps with the endangered Stephens kangaroo rat (*Dipodomys stephensi*) more broadly in the Perris Plain south to Temecula, and lastly switches in the upper Santa Margarita Watershed near Aguanga and overlaps *Dipodomys merriami collinus* and tracks the range of this subspecies into San Felipe Creek ([Lidicker 1960](#)) and then south into Mason Valley. Farther south, *P. l. brevinasus* overlaps *Dipodomys merriami trinidadensis* possibly in the Jacumba Valley. This overlap with three different subspecies of *Dipodomys merriami* is worth further investigation, as these overlap combinations coincide with several of the evolutionary hotspots identified in [Vandergast *et al.* (2008)](#).

5-Coastal dunes, washes, and marine terraces: This is a complex of geologically divergent areas that are tied together by being coastal (with the exception of San Fernando Valley, discussed last), extending along the coastline from Playa del Rey in Los Angeles County to the Tijuana River wash just north of the Mexican border. The areas are/were occupied by *P. l. cantwelli* except the Tijuana site that was occupied by *P. l. pacificus*. There is a set of coastal dunes that extended in patches from north to south with the most extensive being the high El Segundo sand dunes feature. This area was known for extreme endemism in invertebrates ([Mattoni 1992](#)). Most of this feature is now gone except for a 300+ acre portion on Los Angeles World Airways property that is managed as a reserve. Immediately to the south is the prominent feature of Palos Verdes Peninsula that lacks any appropriate habitat for pocket mice. South of these hills is Wilmington, where three specimens were collected in 1865 ([Cooper 1869](#); now MVZ 5633 to 5635). This area comprises large riverine sandy alluvium and low elevation marine terraces that extend to Newport Back Bay. All three major rivers (Los Angeles, San Gabriel, and Santa Ana) once terminated in this region and often flooded a large landscape as they merged during big storm events. This area has not only the earliest record for mice, but subfossil records are known from Huntington Beach (Tom Wake, pers. comm.); the region is now almost entirely developed.

South of Newport Bay are the San Joaquin Hills where pocket mice have occupied patchy, specific marine terrace features ([M'Closkey 1972](#); [Meserve 1976](#); no museum vouchers exist for these sites). Much of this landscape is now protected but the likely mouse habitats are now housing developments. These hills continue south to Dana Point where pocket mice still persist on top of a small coastal bluff on a paleobeach habitat surrounded by housing ([Brehme *et al.* 2021](#)). South of there the mice occurred in patches in Camp Pendleton on other paleobeach formations ([Brehme *et al.* 2017](#)) and then were common on the sand dune for-

mation on the north side of Oceanside where Bailey (1939) was easily able to capture mice by digging them out of the sand. South of Oceanside there are a few possible records and some paleorecords but no museum vouchers until the Tijuana Estuary where *P. l. pacificus* was apparently endemic. This population was discovered in 1894 by E. A. Mearns and F. X. Holzner but not found again until J. C. von Bloeker rediscovered them in July 1931 on river bottom sand (von Bloeker 1931a). Previous effort centered on the small mesa-tops by the international border based on Mearns' locality description. At the time of rediscovery in the river valley, mice were abundant and easily collected but abruptly disappeared within a year or so. They have not been documented from this general area for over 90 years. The river valley is very dynamic and experiences large flood events but also became extensively cultivated (Safran *et al.* 2017). Small patches of native habitat still occur there with appropriate forbland species that *P. l. pacificus* and *P. l. cantwelli* prefer (see von Bloeker 1931a, b; Iwanowicvz *et al.* 2016). Historical reconstructions of the pre-development habitats based on the mid-1800's survey maps, in part, show extensive river wash/riparian scrub habitats that *P. l. pacificus* could have occupied in this valley; Safran *et al.* (2017) estimate this was approximately 1,800 hectares, with 89 % of this habitat lost to date. Additionally, the Pleistocene (glacial maximum) extent of sandy habitats extended well offshore heading towards Coronado Canyon, ~15 km west of the current Tijuana Estuary dune system, greatly extending the potential *P. l. pacificus* habitats historically available in this area (Graham *et al.* 2003).

Lastly, we have the isolated population in the upper Los Angeles River tributary of Big Tujunga wash. This very sandy wash bisected the San Fernando Valley and historically *P. l. cantwelli* here were probably continuous along the Los Angeles River as it passed Burbank and headed south into the Los Angeles Basin. As discussed below, much of this basin habitat was broadly underwater for months in the 1860s due to massive flooding, resulting in likely periodic extirpations of populations of low elevation mice. The upper section in San Fernando Valley apparently persisted until the entire area became urbanized. Recent surveys in the Hansen Dam area in sandy soils in lower Big Tujunga wash have failed to detect this species (Hitchcock *et al.* 2022).

We end this section posing two questions: First, why is *P. longimembris* lacking from the washes connecting the inland alluvial fans and the coastline dunes and terraces? Surprisingly there is a big gap in many species distributions between the coastal zone and inland occurrences in the upper watersheds of the main Los Angeles Basin drainages, exemplified by the subspecies of the giant fly *Rhaphiomidas terminatus*, where one is endemic in the El Segundo sand dunes and the other is endemic inland in the Colton dune system (George and Mattoni 2006), a contrast similar to the current distribution of *P. l. cantwelli* and *P. l. brevinasus*. This appears to be the result of a combination of potential historic and current events. Historic events like the 100

and 1,000 year flood events (in particular the1862 flood; Engstrom 1996) drove the shape and structure of the Los Angeles, San Gabriel, and Santa Ana river washes and the flooding of the Los Angeles Basin. Higher areas of marine terraces and hills like San Joaquin Hills and El Segundo dunes must have been important for long term persistence of the psammophilus species, including the mice, by acting as island refugia. The San Fernando Valley records for *P. l. cantwelli* are thus quite important in showing that this taxon remained connected upstream towards the alluvial fan of Big Tujunga Wash as the San Fernando Valley did not flood during the 1862 event (see Figure 1 in Engstrom 1996) and persisted there at least until the 1930s. Cooper's specimens from Wilmington in 1865 for *P. l. cantwelli* post-date the 1862 flood, so while the landscape was likely inundated by the flood event (Cooper 1869, Engstrom 1996), clearly not all mouse habitat was lost. Currently the areas between coastal occurrences of the mice and inland alluvial fans are primarily urbanized and lack almost any suitable habitats.

Second, why are there two different coastal mice in southern California? Multiple studies of wide-ranging species show that the coastal occurrences of these species at El Segundo dunes are independent lineages from other dunes in southern California, including dunes to the north (Dupuis *et al.* 2020) or those to the south such as the Tijuana River wash (Vandergast *et al.* 2008; Leache *et al.* 2009; Parham and Papenfuss 2009). There are a few species that are coastal dune specific specialists that only occur along the coast; beetles and spiders have, in particular, been studied phylogenetically in this context. These studies show that there is typically isolation by distance in the respective groups with potential north-south speciation between some sets of populations (Bond *et al.* 2001; Chatzimanolis and Caterino 2008). Chatzimanolis and Caternino (2008) stated "It is evident that all the dune systems studied harbor great genetic diversity and the protection of one system cannot act as a surrogate for another." Thus, the finding of two similar but different coastal mice, *pacificus* and *cantwelli*, is not surprising but has important evolutionary and conservation implications.

The lament. Close to 28 million people live in southern California and northern Baja California today. As a consequence, this great diversity of pocket mice has been, and continues to be exposed to many stressors. Although these taxa occur in very different habitats, several of them are threatened by the same factors that will likely impact their long-term persistence. Many of these threats have been identified in various planning documents, such as the recovery plan for the Pacific pocket mouse (U.S. Fish and Wildlife Service 1998), and various actions, such as reserve planning (Chase *et al.* 2000; Barrows *et al.* 2011; Miller *et al.* 2017) and management (Brehme *et al.* 2017; Miller *et al.* 2017; Brehme *et al.* 2021), are helping to mitigate and manage for these stressors. Critically, the Central Coastal NCCP, Western Riverside County MSHCP, Coachella Valley MSCP, SBVWCD, and other entities such as the Camp Pendleton

MCB INRMP all work towards these goals (Chase *et al.* 2000; U.S. Fish and Wildlife Service 2010; Barrows *et al.* 2011; Chock *et al.* 2022). We include a potential threats matrix (Table 1) as a useful platform for continued conservation planning for these taxa and the habitats in which they occur (Miller *et al.* 2017). Sadly, our evidence that *Perognathus l. pacificus* as we define it here (as opposed to recent taxonomy) was endemic to only the Tijuana Watershed and has not been detected since the 1930's supports that this is now the third subspecies of mammal endemic to southern California that is now extinct. Thus, *P. l. pacificus* joins *Perognathus a. alticola* and *Vulpes m. macrotis* as a previously localized endemic in this dynamic and complex habitat to befall the same fate (Davis *et al.* 2008).

We en d on the hopeful note that populations of *P. l. cantwelli* (as defined here as opposed to recent taxonomy in which these populations were considered *P. l. pacificus*) are the focus of conservation efforts by various agencies and landowners (*e. g.*, U.S. Fish and Wildlife Service 2010; Brehme *et al.* 2017; Miller *et al.* 2017; Brehme *et al.* 2021; Chock *et al.* 2022). First collected in 1901 by Frank Stephens (at San Onofre), viable populations remained in the Oceanside area at least until the late 1930s, and continue, as noted above, at sites on Camp Pendleton and at Dana Point. This animal was special to Vernon Bailey, one of the most eminent mammalogists and naturalists of the early 20th century, who kept a pair at his home in Washington, D.C. Below is a poem, penned by Bailey and edited by his wife, Florence Merriam Bailey, about "Bobbity," their name for the mouse that lived the longest. One of us (RNF) found this document, along with an accompanying set of photographs with Bailey's hand-written notes (Figure 12) in the archives of the National Museum of Natural History, Smithsonian Institution, Washington, D.C.

Bobbity

Dear little mouse with shiny coat

Bright black eyes and dainty hands

Watching us with a wistful look

And a far away gaze that understands

More than we think of our intent

And more than we know of distant lands.

Deserts and wastes of sandy soil

Where treasures of seeds in a cool deep cell,

The rich rewards of nights of toil

With the dainty foods that pleased him well.

But when he came to share our life

And freely his valued trust to give

To accept from our hands protection and care

And teach us how his people live

It was only for us to understand

And write his life with a friendly hand.

Acknowledgments

Table 1. Threat assessments that are currently or are likely to impact each of the six subspecies of *Perognathus longimembris* we recognize within the greater southern California-northern Baja California region.

Potential Threats	*pacificus*	*cantwelli*	*brevinasus*	*bangsi*	*arenicola*	*aestivus*
Agriculture[1]	X	X	X	X	X	X
Argentine ants[2]	X	X	X			
Red imported fire ants[3]		X	X	X		
Solar development[4]			X	X	X	
Wind development[5]			X	X	X	
Invasive plants[6]	X	X	X	X	X	X
House cats[7]	X	X	X			
Invasive red fox[8]		X				
Mining[1]					X	
Off-highway vehicles[9]			X	X	X	X
Urbanization[10]	X	X	X	X		
Flooding[11]	X	X	X	X		
Light pollution[12]	X	X	X	X		
Connectivity loss[13]	X	X	X	X		

[1]Lovich and Bainbridge 1999; [2]Laakkonen *et al*. 2001; [3]Allen *et al*. 2004; [4]Lovich and Ennen 2011; [5]Lovich and Ennen 2013; [6]Ceradini and Falfoun 2017; [7]Longcore *et al*. 2009; [8]Golightly *et al*. 1994; [9]Brooks 1995; [10]Amburgey *et al*. 2021; [11]Engstrom 1996; [12]Kotler 1984; [13]Barrows *et al*. 2011.

Literature cited

ABRAMOFF, M. D., P. J. MAGALHAES, AND S. J. RAM. 2004. Image processing with ImageJ. Biophotonics International 11:36-42.

ALLEN, C. R., D. M. EPPERSON, AND A. S. GARMESTANI. 2004. Red imported fire ant impacts on wildlife: a decade of research. American Midland Naturalist 152:88-103.

ÁLVAREZ-CASTAÑEDA, S. T., W. Z. LIDICKER, JR, AND E. RIOS. 2009. Revision of the *Dipodomys merriami* complex in the Baja California Peninsula, Mexico. Journal of Mammalogy 90:992-1008.

AMBURGEY, S. M., ET AL. 2021. The influence of species life history and distribution characteristics on species responses to habitat fragmentation in an urban landscape. Journal of Animal Ecology 90:685-697.

BAILEY, V. 1939. The solitary lives of two little pocket mice. Journal of Mammalogy 20:325-328.

BARROWS, C. W., K. D. FLEMING, AND M. F. ALLEN. 2011. Identifying habitat linkages to maintain connectivity for corridor dwellers in a fragmented landscape. Journal of Wildlife Management 75:682-691.

BOND, J. E., ET AL. 2001. Deep molecular divergence in the absence of morphological and ecological change in the Californian coastal dune endemic trapdoor spider *Aptostichus simus*. Molecular Ecology 10:899-910.

BOOKSTEIN, F. L. 1991. Morphometric tools for landmark data: geometry and biology. Cambridge University Press. New York, U.S.A.

BREHME, C. S., ET AL. 2017. Marine corps base, Camp Pendleton Pacific pocket mouse monitoring results for 2016: 5-year trend analysis and monitoring program evaluation. MCB, Camp Pendleton. DRAFT Prepared for Environmental Security Department, Marine Corps Base, Camp Pendelton, U.S.A.

BREHME, C. S., ET AL. 2021. Dana Point headlands (CNLM, City of Dana Point) Pacific pocket mouse monitoring results for 2020. USGS Cooperator Report to U.S. Fish and Wildlife Service, Carlsbad, U.S.A.

BROOKS, M. L. 1995. Benefits of protective fencing to plant and rodent communities of the western Mojave Desert, California. Environmental Management 19:65-74.

BUISING, A. V. 1990. The Bouse Formation and bracketing units, southeastern California and western Arizona: Implications for the evolution of the proto-Gulf of California and the lower Colorado River. Journal of Geophysical Research 95:20111-20132.

CALIFORNIA NATURAL DIVERSITY DATABASE (CNDDB). July 2022. Special Animals List. California Department of Fish and Wildlife, Sacramento. California, U.S.A.

CERADINI, J. P., AND A. D. CHALFOUN. 2017. Species' traits help predict small mammal responses to habitat homogenization by an invasive grass. Ecological Applications 27:1451-1465.

CHASE, M. K., ET AL. 2000. Single species as indicators of species richness and composition in California coastal sage scrub birds and small mammals. Conservation Biology 14:474-487.

CHATZIMANOLIS, S., AND M. S. CATERINO. 2008. Phylogeography of the darkling beetle *Coelus ciliates* in California. Annals Entomological Society of America 101:939-949.

CHOCK, R. Y., ET AL. 2022. Quantitative SWOT analysis: A structured and collaborative approach to reintroduction site selection for the endangered Pacific pocket mouse. Journal for Nature Conservation 70:126268.

COOPER, J. G. 1869. The naturalist in California. American Naturalist 3:182-189.

DAVIS, E. B., ET AL. 2008. The California hotspots project: identifying regions of rapid diversification of mammals. Molecular Ecology 17:120-138.

DUJARDIN, S., AND J.-P. DUJARDIN. 2019. Geometric morphometrics in the cloud. Infection, Genetics, and Evolution, 70:189-196.

DUPIUS, J. R., ET AL. 2020. Genomics confirms surprising ecological divergence and isolation in an endangered butterfly. Biodiversity and Conservation 29:1897-1921.

Durrant, S. D. 1952. Mammals of Utah, taxonomy and distribution. University of Kansas Publications, Museum of Natural History 6:1-546.

Engstrom, W. N. 1996. The California storm of January 1862. Quaternary Research 46:141-148.

George, J. N., and R. Mattoni. 2006. *Rhaphiomidas terminatus terminatus* Cazier, 1985 (Diptera: Mydidae): notes on the rediscovery and conservation biology of a presumed extinct species. The Pan-Pacific Entomologist 82:30-35.

Golightly, R. T., *et al*. 1994. Food habits and management of introduced red fox in southern California. Proceedings Vertebrate Pest Conference 16:15-20.

Gottscho, A. D. 2016. Zoogeography of the San Andreas Fault system: Great Pacific Fracture Zones correspond with spatially concordant phylogeographic boundaries in western North America. Biological Review 91:235-254.

Gottscho, A. D., *et al*. 2017. Lineage diversification of fringe-toed lizards (Phrynosomatidae: *Uma notata* complex) in the Colorado Desert: delimiting species in the presence of gene flow. Molecular Phylogenetics and Evolution 106:103-117.

Graham, M. H., P. K. Dayton, and J. M. Erlandson. 2003. Ice ages and ecological transitions on temperate coasts. Trends in Ecology and Evolution 18:33-40.

Grinnell, J. 1913. A distributional list of the mammals of California. Proceedings of the California Academy of Sciences, 4th series, 3:265-390.

Grinnell, J. 1914. An account of the mammals and birds of the lower Colorado Valley, with special reference to the distributional problems presented. University of California Publications in Zoology 12:51-294.

Grinnell, J. 1933. Review of the Recent mammal fauna of California. University of California Publications in Zoology 40:71-234.

Grinnell, J., and H. S. Swarth. 1913. An account of the birds and mammals of the San Jacinto area of southern California. University of California Publications in Zoology 10:197-406.

Grismer, L. L. 1994. The origin and evolution of the peninsular herpetofauna of Baja California, Mexico. Herpetological Natural History 2:51-106.

Hafner, D. J. 2016. Subfamily Perognathinae, Genus *Perognathus*. Pp. 202-209, *in* Handbook of mammals of the world, vol. 6, Lagomorphs and Rodents I (Wilson, D. E., T. E. Lacher, Jr., and R. A. Mittermeier, eds.). Lynx Ediciones, Barcelona, Spain.

Hall, E. R. 1941. New heteromyid rodents from Nevada. Proceedings of the Biological Society of Washington 54:55-61.

Hall, E. R. 1946. Mammals of Nevada. University of California Press. Berkeley, U.S.A.

Hall, E. R. 1981. The mammals of North America, vol. 1. John Wiley & Sons. New York, U.S.A.

Hitchcock, C. J., *et al*. 2022. Draft Final: Summary of biodiversity surveys at Hansen Dam Recreational Area, 2020-2021. Report to U.S. Army Corps of Engineers, Los Angeles District, Operations Division.

Hoffmeister, D. F. 1986. Mammals of Arizona. The University of Arizona Press and The Arizona Game and Fish Department, Arizona, U.S.A.

Huey, L. M. 1928. A new silky pocket mouse and a new pocket gopher from Lower California, Mexico. Transactions of the San Diego Society of Natural History 5:87-90.

Huey, L. M. 1939. The silky pocket mice of southern California and northern Lower California, Mexico, with the description of a new race. Transactions of the San Diego Society of Natural History 9:47-54.

Iwanowicz, D. D., *et al*. 2016. Metabarcoding of fecal samples to determine herbivore diets: a case study of the endangered Pacific pocket mouse. Plos One 11:e0165366.

Jockusch, E. L., *et al*. 2020. Slender salamanders (genus *Batrachoseps*) reveal Southern California to be a center for diversification, persistence, and introduction of salamander lineages. PeerJ 8: e9599.

Klingenberg, C. P. 2011. MorphoJ: an integrated software package for geometric morphometrics. Molecular Ecology Resources 11:353-357.

Kotler, B. P. 1984. Effects of illumination on the rate of resource harvesting in a community of desert rodents. American Midland Naturalist 111:383-389.

Laakkonen, J., R. N. Fisher, and T. J. Case. 2001. Effect of land cover, habitat fragmentation and ant colonies on the distribution and abundance of shrews in southern California. Journal of Animal Ecology 70:776-788.

Leaché, A. D., *et al*. 2009. Quantifying ecological, morphological, and genetic variation to delimit species in the coast horned lizard species complex (*Phrysonoma*). Proceedings of the National Academy of Sciences 106:12418-12423.

Lidicker, W. Z., Jr. 1960. An analysis of infraspecific variation in the kangaroo rat *Dipodomys merriami*. University of California Publications in Zoology 67:125-218.

Longcore, T., C. Riche, and L. M. Sullivan. 2009. Critical evaluation of claims regarding management of feral cats by trap-neuter-return. Conservation Biology 23:887-894.

Lovich, J. E., and D. Bainbridge. 1999. Anthropogenic degradation of the Southern California desert ecosystem and prospects for natural recovery and restoration. Environmental Management 24:309-326.

Lovich, J. E., and J. R. Ennen. 2011. Wildlife conservation and solar energy development in the desert southwest, United States. BioScience 61:982-992.

Lovich, J. E., and J. R. Ennen. 2013. Assessing the state of the knowledge of utility-scale wind energy development and operation on non-volant terrestrial and marine wildlife. Applied Energy 103:52-60.

M'closkey, R. T. 1972. Temporal changes in populations and species diversity in a California rodent community. Journal of Mammalogy 53:657-676.

Macmillen, R. E. 1964. Population ecology, water relations, and social behavior of a southern California semidesert rodent fauna. University of California Publications Zoology 71:1-66.

Mattoni, R. H. T. 1992. The endangered El Segundo blue butterfly. Journal of Research on the Lepidoptera 29:277-304.

Mearns, E. A. 1898. Descriptions of three new forms of Pocket-mice from the Mexican border of the United States. Bulletin of the American Museum of Natural History 10:299-302.

Meserve, P. L. 1976. Food relationships of a rodent fauna in a California coastal sage scrub community. Journal of Mammalogy 57:300-319.

Miller, W. B., *et al*. 2017. Little pocket mouse *Perognathus longimembris*. Pp. 85-94, *in* San Diego County Mammal Atlas (Tremor, S., D. Stokes, W. Spencer, J. Diffendorfer, H. Thomas,

S. Chivers, and P. Unitt, eds.). Proceedings of the San Diego Society of Natural History. San Diego, U.S.A.

Mosauer, W. 1932. Adaptive convergence in the sand reptiles of the Sahara and of California: A study of structure and behavior. Copeia 1932:72-78.

Mulcahy, D. G., et al. 2006. Phylogeography of the flat-tailed horned lizard (*Phrynosoma mcallii*) and the systematics of the *P. mcallii-platyrhinos* mtDNA complex. Molecular Ecology 15:1807-1826.

Osgood, W. H. 1900. Revision of the pocket mice of the genus *Perognathus*. North American Fauna 18:9-65.

Osgood, W. H. 1918. The status of *Perognathus longimembris* Coues. Proceedings of the Biological Society of Washington 31:95-96.

Parham, J. F., and T. J. Papenfuss. 2009. High genetic diversity among fossorial lizard populations (*Anniella pulchra*) in a rapidly developing landscape (Central California). Conservation Genetics 10:169-176.

Patton, J. L. 2005. Family Heteromyidae. Pp. 844-858, *in* Mammal species of the world. A taxonomic and geographic reference (Wilson, D. E., and D. E. Reeder, eds.). The Johns Hopkins University Press. Baltimore, U.S.A.

Riddle, B. R., et al. 2000. Cryptic vicariance in the historical assembly of a Baja California Peninsular Desert biota. Proceedings of the National Academy of Sciences (USA) 97:14438-14443.

Riddle, B. R., et al. 2014. Cryptic divergence and revised species taxonomy within the Great Basin pocket mouse, *Perognathus parvus* (Peale, 1848), species group. Journal of Mammalogy 95:9-25.

Rubinoff, D., et al. 2020. Phylogenomics reveals conservation challenges and opportunities for cryptic endangered species in a rapidly disappearing desert ecosystem. Biodiversity and Conservation 29:2185-2200.

Safran, S. M., et al. 2017. Tijuana River Valley historical ecology investigation. Prepared for the state coastal conservancy. San Francisco Estuary Institute-Aquatic Science Center, Richmond. California, U.S.A.

Schneider, C. A., W. S. Rasband, and K. W. Eliceiri. 2012. NIH Image to ImageJ: 25 years of image analysis. Nature Methods 9:671-675.

Stephens, F. 1900. Descriptions of two new mammals from southern California. Proceedings of the Biological Society of Washington 13:153-158.

Swei, A., et al. 2003. Hierarchical genetic structure in fragmented populations of the Little Pocket Mouse (*Perognathus longimembris*) in Southern California. Conservation Genetics 4:510-514.

Tinkham, E. R. 1968. Studies in Nearctic desert sand dune Orthoptera, Part XI. A new arenicolous species of *Stenopelmatus* from Coachella Valley with key and biological notes. Great Basin Naturalist 28:124-131.

USFWS. 1998. Recovery plan for the Pacific pocket mouse (*Perognathus longimembris pacificus*). U.S. Fish and Wildlife Service. Portland, U.S.A.

USFWS. 2010. Pacific pocket mouse (*Perognathus longimembris pacificus*) 5-Year Review: Summary and Evaluation. Carlsbad Fish and Wildlife Office. Carlsbad, U.S.A.

Vandergast, A. G., et al. 2008. Are hotspots of evolutionary potential adequately protected in southern California? Biological Conservation 141:1648-1664.

Von Bloeker, J. C., Jr. 1931a. *Perognathus pacificus* from the type locality. Journal of Mammalogy 12:369-372.

Von Bloeker, J. C., Jr. 1931b. Extension of range of *Perognathus pacificus*. Journal of Mammalogy 12:431-432.

Von Bloeker, J. C., Jr. 1932. A new race of *Perognathus longimembris* from southern California. Proceedings of the Biological Society of Washington 45:127-130.

Wilder. A. P., et al. 2022. A chromosome-length reference genome for the endangered Pacific pocket mouse reveals recent inbreeding in a historically large population. Genome Biology and Evolution https://doi.org/10.1093/gbe/evac122.

Williams, D. F., H. H. Genoways, and J. K. Braun. 1993. Taxonomy. Pp. 38-196 in Biology of the Heteromyidae (Genoways, H. H., and J. H. Brown, eds.). Special Publication No. 10, American Society of Mammalogists. Lawrence, U.S.A.

Wood, D. A., et al. 2008. Molecular and phenotypic diversity in *Chionactis occipitalis* (Western shovel-nosed snake), with emphasis on the status of *C. o. klauberi* (Tucson shovel-nosed snake). Conservation Genetics 9:1489-1507.

Wood, D. A., et al. 2013. Comparative phylogeography reveals deep lineages and regional evolutionary hotspots in the Mojave and Sonoran Deserts. Diversity and Distributions 19:722-737.

Wood, D. A., R. N. Fisher, and A. G. Vandergast. 2014. Fuzzy boundaries: color and gene flow patterns among parapatric lineages of the western shovel-nosed snake and taxonomic implication. Plos One 9:e97494.

Appendix 1

List of measured specimens organized by the sample groups mapped in Figure 1. Sample sizes for each group are given separately for shape and distance data for the dorsal and ventral aspects of the skull ($n_{shape-d}$, $n_{shape-v}$, $n_{distance-d}$, $n_{distance-v}$) and dorsal color (n_c). The total sample sizes, museum acronyms, and catalog numbers are given for each locality, even if some individuals were not included in every analysis. Specimens not assigned to a sample group are listed at the end as unknown.

aestivus ($n_{shape-d}$ = 19, $n_{shape-v}$ = 19, $n_{distance-d}$ = 20, $n_{distance-v}$ = 19, n_c = 8)

MEXICO.—Baja California; Sangre de Cristo (*n* = 5, SDNHM 6050-1, 6098, 6120, 22079); Sangre de Cristo, Valley San Rafael (*n* = 1, SDNHM 6110 [holotype of *aestivus* Huey]); Valle de la Trinidad (*n* = 9, SDNHM 6208, 6323, 6338, 11504, 11642, 11643, 11664-11666); Valle de la Trinidad, Aguajito Spring (*n* = 4, SDNHM 11563, 11591-11593); Valley La Trinidad, La Zapopita (*n* = 1, LACM 13677) – total *n* = 20.

bangsi-1 ($n_{shape-d}$ = 17, $n_{shape-v}$ = 15, $n_{distance-d}$ = 22, $n_{distance-v}$ = 23, n_c = 1)

CALIFORNIA.—Riverside Co.; Colorado Desert, Dos Palmas (*n* = 1, LACM 4346); Desert Center, 9.4 mi S, 9.8 mi W; Salt Creek Wash (*n* = 21, LACM 80544-80549, 85070, 86352, 86354-86361, 86363-86364, 86366, 86369); 0.2 mi W Rancho Dos Palmas (*n* = 1, MVZ 195955); Shavers Valley, ca. 9 mi E Cactus City (*n* = 1, MVZ 195954) – total *n* = 24.

bangsi-2 ($n_{shape-d}$ = 32, $n_{shape-v}$ = 30, $n_{distance-d}$ = 34, $n_{distance-v}$ = 32, n_c = 27)

CALIFORNIA.—Riverside Co.; Garnet (*n* = 2, MVZ 90652, 90655); Indio Hills, Pushawalla Canyon, 3.5 mi NW junction of Berdoo Canyon road and Dillon road (*n* = 1, MVZ 184650); Palm Springs (*n* = 14, MCZ 5304 [holotype of *bangsi* Mearns]; LACM 3233, 3291, 3294-3295, 3298, 30072; MVZ 31839; SBMNH 6663-6664, 6666; SDNHM 6666-6667, 22081); Palm Springs, 5 mi NW (*n* = 1, LACM 10352); Santa Rosa Mts.; Deep Canyon (*n* = 1, LACM 20676); 3 mi E Thousand Palms (*n* = 1, LACM 90123); 2.5 mi E and 0.5 mi S Whitewater (*n* = 6, MVZ 85064-85069); 2.5 mi E and 1 mi S Whitewater (*n* = 12, MVZ 85050-85057, 85060-85063) – total *n* = 38.

bangsi-3 ($n_{shape-d}$ = 41, $n_{shape-v}$ = 37, $n_{distance-d}$ = 41, $n_{distance-v}$ = 37, n_c = 20)

CALIFORNIA.—Riverside Co.; 5 mi E Cabezon (*n* = 8, MVZ 84352-84357, 84373-84374); 7 mi E and 1.2 mi S Cabezon (*n* = 2, MVZ 84358, 84360); 0.5 mi W and 0.1 mi S Palm Springs Station (*n* = 1, MVZ 184651); 2 mi W Palm Springs Station (*n* = 1, MVZ 84363); San Gorgonio River, 0.33 mi S, 0.41 mi W Whitewater (*n* = 7, LACM 80550-80556); Snow Creek, near Whitewater (*n* = 11, MVZ 1471, 1473-1474, 1485-1486, 1492-1493, 1495, 1497, 1499, 1502); 0.95 mi S hwy 111 on Snow Creek Road (*n* = 10, MVZ 184653-184662); Whitewater Station (*n* = 1, MVZ 1506); 0.5 mi S and 0.8 mi W Whitewater (*n* = 3, MVZ 206791-206793) – total *n* = 44.

bangsi-4 ($n_{shape-d}$ = 63, $n_{shape-v}$ = 60, $n_{distance-d}$ = 64, $n_{distance-v}$ = 61, n_c = 76)

CALIFORNIA.—Riverside Co.; Cabazon (*n* = 68, LACM 2259, 20505, 20526-20531; SBMNH 6671-6672; SDNHM 5610, 5615-5622, 5624, 5633-5637, 5639-5644, 5653-5661, 5672-5677, 5679-5680, 5686-5689, 7302-7304, 7325-7328, 7341-7343, 7345-7346; USNM 54075-54077); 0.25 mi E Cabazon (*n* = 2, MVZ 90653-90654); 0.5 mi E Cabazon (*n* = 1, MVZ 90654); 1 mi E Cabazon (*n* = 6, MVZ 184645-184649, 195956); 1 mi S Cabazon (*n* = 3, LACM 10360-10362); 2 mi S Cabazon (*n* = 7, LACM 10354-10359); 2 mi W and 1 mi N Cabazon (*n* = 2, MVZ 84347-84348) – total *n* = 89.

bangsi-5 ($n_{shape-d}$ = 11, $n_{shape-v}$ = 11, $n_{distance-d}$ = 11, $n_{distance-v}$ = 11, n_c = 23)

CALIFORNIA.—Riverside Co.; Banning (*n* = 1, USNM 160083); Banning, base of San Jacinto Mts (*n* = 2, MVZ 1489-1490); base of San Jacinto Mts, near Cabazon (*n* = 2, MVZ 1367, 1378); 2 mi W and 1 mi N Cabezon (*n* = 1, MVZ 84349); 2 mi W and 1.5 mi N Cabezon (*n* = 2, MVZ 84346-84347); base San Jacinto Mts, near Cabazon (*n* = 13, MVZ 1356-1363, 1366-1367, 1378-1380); San Jacinto Mts., near Cabazon (*n* = 7, MVZ 1370, 1372-1377) – total *n* = 28.

bangsi-6 ($n_{shape-d}$ = 28, $n_{shape-v}$ = 24, $n_{distance-d}$ = 27, $n_{distance-v}$ = 27, n_c = 31)

CALIFORNIA.—San Diego Co.; Borrego Springs, 3 mi S, 3.5 mi W (*n* = 4, LACM 38499-38502); below Borrego Springs (*n* = 3, SDNHM 915-916, 918); 3.3 mi S Borrego Springs on hwy 53 (*n* = 1, MVZ 184663); 4 mi S Borrego Springs (*n* = 1, LACM 69588); 10 mi E Borrego Springs (*n* = 1, SDNHM 917); Borrego Valley, Beatty Ranch (*n* = 17, LACM 3039-3055); Borrego Valley, mouth of Coyote Creek (*n* = 4, LACM 29355-29359); Borrego Valley, Palm Canyon (*n* = 3, LACM 3036-3038); Borrego Valley, 3 mi SW Palm Canyon (*n* = 1, SBMHN 6662); Culp Valley, 2 mi E Ranchita (*n* = 1, SDMNHM) – total *n* = 36.

bangsi-7 ($n_{shape-d}$ = 43, $n_{shape-v}$ = 39, $n_{distance-d}$ = 42, $n_{distance-v}$ = 38, n_c = 43)

CALIFORNIA.—San Diego Co.; San Felipe Narrows (*n* = 43, LACM 3032-3035, 3171-3186; MVZ 55156; SBMNH 6645-6661; SDNHM 1590, 2625, 2627-2628, 6661, 17621, 19211; USNM 99828 [holotype of *arenicola* Stephens]); San Felipe Narrows, Desert Sand Dunes (*n* = 1, UAZ 17143); E side San Felipe Narrows (*n* = 4; SDNHM 9911-9913, 9923) – total *n* = 48.

bangsi-8 ($n_{shape-d}$ = 13, $n_{shape-v}$ = 13, $n_{distance-d}$ = 12, $n_{distance-v}$ = 13, n_c = 3)

MEXICO.—Baja California; Cerro Centinela, 12 mi WSW Mexicali (*n* = 1, MVZ 111306). CALIFORNIA.—Imperial Co.; Crucifixion Thorn Reserve, 0.8 mi S and 7.8 mi E Ocotillo (*n* = 1, MVZ 184644); 3.2 mi W Ocotillo, 0.2 mi S hwy 52; Dos Cabezas Rd (*n* = 3, LACM 46578-46580); Yuha, Smoke Tree Wash (*n* = 10, LACM 65147-65153, 65165, 80014-80015) – total *n* = 15.

Appendix 1
Continuation

bombycinus-1 ($n_{shape-d}$ = 6, $n_{shape-v}$ = 6, $n_{distance-d}$ = 6, $n_{distance-v}$ = 5, n_c = 1)

CALIFORNIA.—Riverside Co.; 9 mi W Blythe (*n* = 1, LACM 4189); 6.5 mi NW Blythe (*n* = 1, MVZ 239809); 26 mi W Blythe; Chuckwalla Rd; I-10, 4 mi W (*n* = 3, LACM 80540-80542); Chuckwalla Valley, 2 mi S, 19 mi W Blythe (*n* = 1, LACM 80543); Hopkins Well (*n* = 1, LACM 7594) – total *n* = 7.

bombycinus-2 ($n_{shape-d}$ = 15, $n_{shape-v}$ = 7, $n_{distance-d}$ = 15, $n_{distance-v}$ = 7, n_c = 3)

CALIFORNIA.—Imperial Co.; Colorado River, Pilot Knob (*n* = 1, MVZ 9976); Colorado River near Pilot Knob (*n* = 3, MVZ 9973-9975); 8.6 mi W, 0.6 mi N Glamis (*n* = 5, UAZ 11185-11188, 15353); 21 mi N Glamis (*n* = 1, UAZ 11299); west side Pilot Knob (*n* = 1, MVZ 239808); 3 mi W Pilot Knob (*n* = 2, SDNHM 4532-4533); 2 mi N I-8 on county hwy S-34 (*n* = 2, MSB 190591-190592) – total *n* = 15.

brevinasus-1 ($n_{shape-d}$ = 53, $n_{shape-v}$ = 48, $n_{distance-d}$ = 53, $n_{distance-v}$ = 48, n_c = 29)

CALIFORNIA.—Riverside Co.; Reche Canyon (*n* = 1, SDNHM 19212). San Bernardino Co.; mouth of Reche Canyon, near Colton (*n* = 1, MVZ 2656); Reche Canyon, 4 mi SE Colton (*n* = 1, MVZ 24496); San Bernardino (*n* = 22, SDNHM 908-909), USNM 22630-22631, 22634, 186515 [holotype of *brevinasus* Osgood], 192214, 192223-192226, 192230, 192233-192234, 192240-192244, 192248-192249); 4.75 mi N San Bernardino (*n* = 3, MVZ 77112-77114); 5 mi NW San Bernardino (*n* = 26, SDNHM 13311-13312, 13314, 13316, 13318-13322, 13328-13339, 13342, 13344-13347); Slover Mt near Colton (*n* = 1, MVZ 16664) – total *n* = 55.

brevinasus-2 ($n_{shape-d}$ = 18, $n_{shape-v}$ = 16, $n_{distance-d}$ = 17, $n_{distance-v}$ = 13, n_c = 21)

CALIFORNIA.—Riverside Co.; Menifee (*n* = 16, LACM 2649-2655, 3997-4006); 1 mi E Menifee (*n* = 1, LACM 48842); Winchester (*n* = 3, LACM 3655-3657); 1.5 mi W Winchester (*n* = 1, LACM 48841) – total *n* = 21.

brevinasus-3 ($n_{shape-d}$ = 10, $n_{shape-v}$ = 7, $n_{distance-d}$ = 9, $n_{distance-v}$ = 8, n_c = 11)

CALIFORNIA.—Riverside Co.; Aguanga (*n* = 2, SDNHM 1780, 13361); 0.25 mi ENE Aguanga (*n* = 1, MVZ 123341); 5 mi N 0.25 mi W Aguanga (*n* = 3, LACM 48843-48845). San Diego Co.; Oak Grove, N side Palomar Mt (*n* = 1, SBMNH 6673); 2.5 mi N Oak Grove (*n* = 6, SDNHM 13369-13374) – total *n* = 13.

internationalis-1 ($n_{shape-d}$ = 42, $n_{shape-v}$ = 42, $n_{distance-d}$ = 43, $n_{distance-v}$ = 43, n_c = 39)

MEXICO.—Baja California; international boundary near Jacumba, CA (*n* = 38, SDNHM 11917-11936, 11944-11957, 11970, 11971 [holotype of *internationalis* Huey], 11972-11973). CALIFORNIA.—San Diego Co.; Jacunta [= Jacumba] (*n* = 1, FMNH 6984); Jacumba, 12 mi N, 4.5 mi E, old hwy 80 (*n* = 2, LACM 81008-81009); Jacumba Range, Smugglers Cave Basin (*n* = 1, LACM 46800); I-8, 4.2 mi N, In-Ko-Pah Valley Rd (*n* = 3, LACM 81005-81007) – total *n* = 45.

internationalis-2 ($n_{shape-d}$ = 31, $n_{shape-v}$ = 23, $n_{distance-d}$ = 31, $n_{distance-v}$ = 22, n_c = 29)

CALIFORNIA.—San Diego Co.; La Puerta Valley (*n* = 33, SBMNH 6674-6680, 6682); SDNHM 1416-1417, 1424, 1431-1432, 1850, 1860, 1866, 1910, 2168, 2198, 2204, 2207, 2214-2217, 2220-2223, 2237, 2256, 2266, 7174, 20398-20399); La Puerta Valley [= Mason Valley] (*n* = 5, MVZ 18847, 18849, 32834, 32836, 32838) – total *n* = 38.

internationalis-3 ($n_{shape-d}$ = 19, $n_{shape-v}$ = 11, $n_{distance-d}$ = 19, $n_{distance-v}$ = 11, n_c = 16)

CALIFORNIA.—San Diego Co.; 5.5 mi N Banner, San Felipe Valley (*n* = 2, MVZ 122457-122458); Coast Range Mountains, Summit (*n* = 1, USNM 60718); Julian, 1 mi N, 7.3 mi E, Scissors Crossing [Earthquake Valley] (*n* = 2, LACM 89253-89254); San Felipe Valley (*n* = 2, MVZ 7541; SDNHM 913); Scissor's Crossing, Earthquake Valley (*n* = 9, MVZ 123345-123354); 3.25 mi S, 3.25 mi E Scissor Crossing, Earthquake Valley (*n* = 4, MVZ 123355-123358) – total *n* = 20.

pacificus-1 ($n_{shape-d}$ = 63, $n_{shape-v}$ = 61, $n_{distance-d}$ = 66, $n_{distance-v}$ = 63, n_c = 35)

CALIFORNIA.—San Diego Co.; Mexican Boundary Monument No. 258, edge of Pacific Ocean at Mexican Boundary Monument No. 258 (*n* = 1, USNM 61022 [holotype of *pacificus* Mearns]); Mexican Boundary Monument No. 258, shore of Pacific Ocean (*n* = 1, USNM 61024); 2 mi N Monument #258, mouth of Tijuana River (*n* = 12, LACM 2702-2705, 2707-2713, 2718); near mouth Tijuana River (*n* = 4, MVZ 47312-47313; SDNHM 19213, 19216); Tijuana River (*n* = 1, SDNHM 9712); Tijuana River; mouth, 2 mi N Monument #258 (*n* = 11, SBMNH 6691, 6693-6694, 6697-6698, 6701, 6703-6704, 6707-6708, 6710); Tijuana River Valley (*n* = 8, SDNHN 22085, 22088, 22408-22413); Tijuana Valley (*n* = 35, SDNHM 9510-9512, 9717-9721, 9724, 9727-9732, 9741-9745, 9747, 9749-9753, 9756-9757, 9762-9765, 9767, 9774, 9775, 10562); US-Mexico border, Monument 258 (*n* = 1, SBMNH 6806) – total *n* = 72.

pacificus-2 ($n_{shape-d}$ = 48, $n_{shape-v}$ = 40, $n_{distance-d}$ = 48, $n_{distance-v}$ = 42, n_c = 25)

CALIFORNIA.—Orange Co.; Dana Point (*n* = 1, MVZ 195949); Dana Pt, 5 mi W Capistrano Beach (*n* = 8, LACM 3282-3289). San Diego Co.; Oceanside (*n* = 28, LACM 3562-3563; MVZ 47101-47103, 47105-47106; SBMNH 6804; SDNHM 16222-

Appendix 1
Continuation

16224, 16226-16229, 16233-16235, 16238-16239, 16241-16243, 17614-17615, 17617, 17620, 18705); 4 mi N Oceanside (n = 4, SDNHM 10595-10597, 10599); 4 mi NW Oceanside; Santa Margarita Ranch (n = 6, LACM 2720-2727); Oscar One Training Area, Camp Pendleton Marine Corps Base (n = 7, MVZ 195952); San Onofre (n = 1, SDNHM 923); San Onofre Creek, dry mesa at mouth (n = 1, SBMNH 6711); San Onofre, 2 mi E on hwy 101 (n = 1, SBMNH 6712); Santa Margarita River, 5 mi N Oceanside (n = 6, SBMNH 6713-6718) – total n = 63.

pacificus-3 ($n_{shape-d}$ = 80, $n_{shape-v}$ = 75, $n_{distance-d}$ = 77, $n_{distance-v}$ = 76, n_c = 92)

CALIFORNIA.—Los Angeles Co.; Clifton (n = 2, SBMNH 6737-6738); Del Rey (n = 9, LACM 3220-3228, 3233); Del Rey Hills, near Loyola University (n = 3, LACM 4486-4488); 0.5 mi NW El Segundo (n = 1, MVZ 74750); 1 mi N El Segundo (n = 5 , SDNHM 13349-13350, 13352, 13354-13355); Hyperion (n = 79, LACM 429; SBMNH 6719-6720, 6726-6736, 6740-6802); Hyperion [= El Segundo] (n = 2, MVZ 74680 [holotype of *cantwelli* von Bloeker]; UAZ 17145), Palisades Del Rey (n = 1, SBMNH 6723); Playa del Rey (n = 9, LACM 3529, 3727-3729, 4382, 48822-48825) – total n = 102.

unknown ($n_{shape-d}$ = 24, n_c = 26)

CALIFORNIA.—Imperial Co.; Salton Sea (n = 1, LACM 65146). Los Angeles Co.; San Fernando (n = 3, SBMNH 6667-6669). Riverside Co.; Dos Palmas Spring, Santa Rosa Mts (n = 2, MVZ 1929-1930); Eden Hot Springs (n = 1, MVZ 90713); Hemet (n = 1, USNM 149899); Santa Rosa Mts, 0.4 mi E Dos Palmas Spring (n = 1, MVZ 184652); Temecula, at I-15 hwy 79 jct, Santa Gertrudis Creek (n = 1, LACM 80249); near Temecula, Rancho California Valley (n = 1, LACM 89250); Vallevista, San Jacinto Valley (n = 7, MVZ 2278-2281, 2283-2285). San Diego Co.; 3.25 mi N Manzanita, McCain Valley (n = 2, MVZ 123359-123360); Warner Pass (n = 14, MVZ 7620-7629, 7660-7662, 7666) – total n = 34.

Appendix 2

Main effects of sex, age, and paired interaction in a least squares analysis of the pooled pacificus-1 (*pacificus* Mearns) and pacific-3 (*cantwelli* von Bloeker) samples (*n* = 66 and 78, respectively) for cranial variables; only *P*-values are provided, significant ones in bold (Bonferroni corrected *P* at $\alpha_{0.05}$ = 0.0016).

Sample	Pacificus-1 [pacificus]			Pacificus-3 [cantwelli]		
	n = 66			*n* = 78		
Aariable	Sex	Age	Sex * age	Sex	Age	Sex * age
Dorsal measurements						
occipito-nasal length	0.306	0.027	0.036	0.159	0.645	0.519
nasal length	0.179	**0.001**	0.020	0.248	0.489	0.604
frontal length	0.488	0.349	0.469	0.471	0.692	0.388
parietal length	0.900	0.495	0.902	0.061	0.256	0.680
interparietal length	0.447	0.275	0.654	0.334	0.902	0.876
premax-extension length	0.561	0.645	0.970	0.532	0.651	0.214
rostral width	0.397	0.012	0.083	0.400	0.143	0.912
maxillary width	0.985	0.508	0.445	0.876	0.252	0.846
premax-extension width	0.562	0.555	0.850	0.564	0.492	0.928
interorbital constriction	0.060	0.315	0.210	0.462	0.428	0.647
zygomatic breadth	0.050	**0.001**	0.028	0.231	0.045	0.699
parietal width-anterior	0.016	0.359	0.513	0.788	0.301	0.467
interparietal width-anterior	0.690	0.958	0.635	0.714	0.026	0.128
interparietal width-posterior	0.739	0.588	0.504	0.393	0.108	0.441
exoccipital width	0.429	0.124	0.859	0.940	0.749	0.149
bullar width	0.495	0.059	0.059	0.412	0.363	0.374
bulla length	0.871	0.444	0.096	0.292	0.509	0.244
bulla width	0.786	0.336	0.011	0.458	0.039	0.723
bulla area	0.399	0.105	0.031	0.504	0.032	0.651
bulla perimeter	0.762	0.484	0.085	0.173	0.193	0.730
Ventral measurements						
anterior nasal extension	0.807	0.271	0.006	0.013	0.227	0.984
palatal length	0.568	0.005	0.019	0.312	0.158	0.855
mesopterygoid fossa length	0.854	0.380	0.695	0.215	0.593	0.593
foramen magnum length	0.649	0.009	0.257	0.955	0.084	0.436
maxillary toothrow length	0.800	0.643	0.145	0.603	0.849	0.321
upper incisor breadth	0.879	**0.001**	0.185	0.428	0.604	0.569
palatal breadth	0.629	0.006	0.279	0.404	0.243	0.808
squamosal breadth	0.036	0.267	0.083	0.868	0.440	0.135
mesopterygoid width	0.218	**0.001**	0.768	0.675	0.009	0.658
stylomastoid foramina width	0.619	0.166	0.065	0.395	0.072	0.884
occipital condyle width						
	0.665	0.042	0.211	0.501	0.703	0.090
exoccipital width	0.992	0.145	0.760	0.505	0.141	0.929

Appendix 3

External measurements (column A) and selected cranial dimensions (column B) for samples that contain the holotype and topotypic series for each of the seven subspecies described from the study area in southern California and northern Baja California. Data include minimal non-significant subsets based on oneway ANOVAs followed by Tukey-Kramer HSD pairwise tests (with Bonferroni corrected *P*-values for multiple tests), sample mean and standard error (in mm), and sample size. See text for definition of variables.

A: External measurements (from specimen labels)

variable/taxon	A	B	C	D	mean	std err	n
TOL							
internationalis	A				141.76	0.908	38
aestivus	A				141.35	1.357	17
arenicola	A				139.89	0.946	35
brevinasus		B			134.07	1.077	27
bangsi			C		129.50	1.769	10
cantwelli			C		127.62	0.735	58
pacificus				D	119.64	0.754	55
TAL							
arenicola	A				79.03	0.793	35
internationalis	A				77.74	0.761	38
aestivus	A				77.71	1.137	17
bangsi		B			71.00	1.483	10
brevinasus		B			70.00	0.903	27
cantwelli			C		67.45	0.616	58
pacificus				D	61.58	0.632	55
HBL [TOL-TAL]							
brevinasus	A				64.07	0.676	27
internationalis	A				64.03	0.569	38
aestivus	A				63.65	0.851	17
arenicola		B			60.86	0.593	35
cantwelli		B			60.17	0.461	58
bangsi		B	C		58.50	1.110	10
pacificus			C		58.05	0.473	55
TAL:TOL x 100							
arenicola	A				56.47	0.386	35
aestivus		B			54.94	0.554	17
bangsi		B			54.83	0.722	10
internationalis		B			54.82	0.370	38
cantwelli			C		52.80	0.300	58
brevinasus			C	D	52.21	0.439	27
pacificus				D	51.47	0.308	55
HF [w/ claw]							
aestivus	A				18.83	0.145	18
internationalis	A				18.65	0.101	37
arenicola	A				18.63	0.104	35
brevinasus	A				18.52	0.114	29
bangsi	A	B			18.40	0.194	10
cantwelli		B			17.78	0.080	59
pacificus			C		16.76	0.083	55
E [notch]							
internationalis	A				7.03	0.087	37
aestivus	A				6.94	0.124	18
brevinasus	A				6.86	0.098	29
bangsi	A	B			6.67	0.176	9
cantwelli		B	C		6.30	0.083	40
pacificus			C		6.21	0.073	53
arenicola			C		6.10	0.12	21

B: Selected cranial dimensions

variable/taxon	A	B	C	D	E	mean	std err	n
ONL								
aestivus	A					21.57	0.116	55
internationalis		B				21.18	0.081	39
brevinasus		B	C			21.06	0.073	60
bangsi			C			20.84	0.095	48
arenicola				D		20.39	0.083	28
pacificus					E	19.83	0.068	37
cantwelli					E	19.76	0.065	19
NL								
aestivus	A					7.70	0.066	19
bangsi	A					7.67	0.054	28
internationalis	A	B				7.57	0.046	39
brevinasus		B	C			7.49	0.042	48
arenicola			C			7.42	0.047	37
cantwelli				D		6.87	0.037	60
pacificus					E	6.65	0.039	55
RL								
internationalis	A					2.16	0.016	39
aestivus	A	B				2.13	0.022	19
brevinasus	A	B				2.12	0.014	48
bangsi		B	C			2.08	0.018	28
pacificus			C			2.05	0.013	55
cantwelli				D		2.00	0.013	60
arenicola				D		1.98	0.016	37
IOC								
aestivus	A					5.10	0.039	19
internationalis	A	B				5.04	0.028	39
brevinasus		B				5.00	0.025	48
bangsi		B				4.98	0.033	28
pacificus			C			4.81	0.023	55
arenicola				D		4.70	0.028	37
cantwelli				D		4.65	0.022	60
IPW-ant								
brevinasus	A					3.88	0.036	48
pacificus	A					3.85	0.033	55
bangsi	A					3.77	0.047	28
internationalis		B				3.63	0.040	39
cantwelli		B				3.55	0.032	60
arenicola			C			3.10	0.041	37
aestivus			C			3.10	0.057	19
bulla perimeter*								
aestivus	A					21.44	0.162	19
arenicola		B				19.26	0.116	37
internationalis		B				19.09	0.113	39
bangsi			C			18.17	0.133	28
brevinasus			C			17.86	0.102	48
pacificus				D		17.32	0.095	55
cantwelli					E	16.61	0.091	60

* bulla perimeter is strongly correlated with both bulla length ($R^2 = 0.939$) and bulla width ($R^2 = 0.935$)

Appendix 4

Colorimetric variables for 20 sample groups of *Perognathus longimembris* from the study area in southern California and northern Baja California. Data for each variable (L* [Lightness], Chroma, and Hue) include minimal non-significant subsets based on oneway ANOVAs followed by Tukey-Kramer HSD pairwise tests (with Bonferroni corrected *P*-values for multiple tests), sample mean and standard error, and sample size. See text for definition of variables.

Variable/taxon	A	B	C	D	E	F	G	H	I	mean	std err	n
L* [Lightness]												
bangsi-1	A	B								46.53	5.106	1
bangsi-7	A									44.03	0.779	43
bangsi-6	A									42.34	0.917	31
bombycinus-2	A	B								40.42	2.948	3
bangsi-2	A									39.74	0.983	27
bombycinus-1	A	B								39.70	5.106	1
bangsi-8	A	B	C							37.02	2.948	3
bangsi-3		B								32.44	1.142	20
aestivus		B	C	D	E					31.16	1.805	8
bangsi-4		B	C	D						29.89	0.586	76
internationalis-2			C	D	E	F				25.95	0.948	29
brevinasus-3				D	E	F	G			24.77	1.539	11
internationalis-1					E	F				24.34	0.818	39
brevinasus-1						F	G			23.40	0.948	29
brevinasus-2						F	G			22.99	1.114	21
internationalis-3						F	G	H		22.36	1.365	14
bangsi-5						F	G	H		21.62	1.065	23
pacificus-2							G	H	I	18.52	1.021	25
pacificus-3								H	I	17.53	0.532	92
pacificus-1									I	13.99	0.863	35

Variable/taxon	A	B	C	D	E	F	mean	std err	n
Hue									
bangsi-6	A	B					1.27	0.013	31
bangsi-7	A						1.27	0.011	43
bangsi-4	A	B					1.26	0.008	76
aestivus	A	B	C				1.26	0.026	8
bangsi-2	A	B					1.26	0.014	27
bombycinus-2	A	B	C				1.25	0.042	3
bombycinus-1	A	B	C				1.24	0.074	1
bangsi-3	A	B	C				1.24	0.016	20
internationalis-2	A	B	C				1.23	0.014	29
brevinasus-3	A	B	C				1.23	0.022	11
bangsi-1	A	B	C				1.23	0.074	1
internationalis-1	A	B	C				1.23	0.012	39
internationalis-3	A	B	C				1.23	0.020	14
brevinasus-1		B	C				1.21	0.014	29
brevinasus-2		B	C	D			1.20	0.016	21
bangsi-8	A	B	C	D			1.18	0.042	3
bangsi-5			C	D	E		1.17	0.015	23
pacificus-2				D	E	F	1.13	0.015	25
pacificus-3					E	F	1.13	0.008	92
pacificus-1						F	1.08	0.012	35

Variable/taxon	A	B	C	D	E	F	G	H	mean	std err	n
Chroma											
bangsi-1	A	B	C	D					21.86	2.830	1
bombycinus-2	A	B	C	D					21.06	1.634	3
bangsi-2	A								20.16	0.545	27
bangsi-7	A								19.81	0.432	43
aestivus	A	B	C						19.56	1.001	8
bangsi-6	A	B							18.84	0.508	31
bombycinus-1	A	B	C	D					18.69	2.830	1
bangsi-3	A	B	C	D			G		17.87	0.633	20
bangsi-4		B	C				G		17.38	0.325	76
internationalis-2		B	C	D	E		G		17.04	0.525	29
bangsi-8	A	B	C	D	E				16.83	1.634	3
internationalis-3			C	D	E	F	G		15.12	0.756	14
internationalis-1				D	E	F			15.11	0.453	39
brevinasus-1					E	F			14.38	0.525	29
brevinasus-3					E	F	G		14.29	0.853	11
brevinasus-2					E	F			14.17	0.618	21
bangsi-5						F			14.00	0.590	23
pacificus-3						F			13.44	0.295	92
pacificus-2						F			12.73	0.566	25
pacificus-1								H	9.44	0.478	35